Review Article

Deciphering Photoreceptors Through Atomistic Modeling from Light Absorption to Conformational Response

Giacomo Salvadori, Patrizia Mazzeo, Davide Accomasso, Lorenzo Cupellini and Benedetta Mennucci

Department of Chemistry and Industrial Chemistry, *University of Pisa, 56124 Pisa, Italy*

Correspondence to :
https://doi.org/10.1016/j.jmb.2023.168358
Edited by: Volha Chukhutsina

Abstract

In this review, we discuss the successes and challenges of the atomistic modeling of photoreceptors. Throughout our presentation, we integrate explanations of the primary methodological approaches, ranging from quantum mechanical descriptions to classical enhanced sampling methods, all while providing illustrative examples of their practical application to specific systems. To enhance the effectiveness of our analysis, our primary focus has been directed towards the examination of applications across three distinct photoreceptors. These include an example of Blue Light-Using Flavin (BLUF) domains, a bacteriophytochrome, and the orange carotenoid protein (OCP) employed by cyanobacteria for photoprotection. Particular emphasis will be placed on the pivotal role played by the protein matrix in fine-tuning the initial photochemical event within the embedded chromophore. Furthermore, we will investigate how this localized perturbation initiates a cascade of events propagating from the binding pocket throughout the entire protein structure, thanks to the intricate network of interactions between the chromophore and the protein.

Introduction

Light-induced processes in proteins are crucial for various biological functions, including vision, energy production through photosynthesis, and regulation of biological rhythms. Among the light-responsive proteins, the photoreceptors play a major role, allowing the embedding organisms to sense and respond to light in their environment.[1–5] Photoreceptors exhibit diverse behaviors depending on their specific functions, but they share a fundamental characteristic: the presence of a light-absorbing molecule (the chromophore) that initiates the ultimate protein response. To comprehensively understand the entire process, starting from the absorption of light by the chromophore to the protein's response, a detailed atomistic investigation is essential. Coarser-grained descriptions would inevitably overlook some of the fundamental components of the complex network of interactions responsible for transmitting the response effectively.

Over the years, a significant portion of our understanding of photoreceptors and their mechanisms of action has been achieved through the integration of structural and spectroscopic studies.[6,7] Presently, we have access to detailed structural information about numerous photoreceptors, thanks to high-resolution crystallography and cryo-electron microscopy characterizations. Additionally, time-resolved spectroscopic methods have enabled us to track the dynamics of light-induced

processes, providing valuable insights into their functioning. Nevertheless, a comprehensive depiction of the entire process for various types of photoreceptors remains incomplete. In certain instances, the structural characterization is available only for one of the multiple (meta) stable states engaged in the process, or the latter is known only within limited time windows. Thus, there are still gaps in our knowledge, hindering a complete understanding of the intricate workings of the different types of photoreceptors. In this scenario, a highly promising approach to bridge this knowledge gap involves integrating structural and spectroscopic data with atomistic modeling.

However, atomistic modeling faces significant challenges when applied to photoreceptors. Understanding how these receptors function requires bridging the gap between their multiscale spatial characteristics and temporal dynamics. The spatial scale initiates at the level of chromophores, where the absorption of light triggers a photochemical transformation, often involving structural or chemical changes. However, the successful completion of the system's function relies on the effective propagation of this local change throughout the entire protein matrix. In this way, in fact, the protein changes its conformation from the initial (resting) state to the final (active) one. This spatial multiscalarity is intricately linked to a time evolution that spans from the ultrafast femtosecond to picosecond scales of the photochemical event, up to the significantly slower microsecond or even millisecond scales of the protein conformational changes.

In this review, we will present and discuss the recent progress in the atomistic modeling of photoreceptors and their mechanisms of functioning. The aim of this perspective is not solely to provide a critical survey of the principal computational techniques applied in this field, but also to underscore how atomistic simulations can unveil the pivotal role of the protein matrix in selecting the precise photoactivation mechanism and shaping pathways by adjusting energetics and kinetics.

Given the constraints of this review in covering such a large and still expanding field (for more comprehensive reviews, refer to Refs. [8–13]), we will mostly focus on three photoreceptors recently studied within our research group. These include an example of Blue Light-Using Flavin (BLUF) domain, a bacteriophytochrome, and the orange carotenoid protein (OCP). These cytoplasmic proteins serve a range of biological functions. The first belongs to the AppA protein, which functions as a transcriptional antirepressor regulating the expression of genes associated with photosynthesis in the bacterium *Rhodobacter sphaeroides*.[14] Phytochromes control the growth, reproduction, and movement in plants, fungi, and bacteria. The biological function of *Deinococcus radiodurans* phytochrome includes photoregulation of gene expression, phototaxis, and adaptation to harsh environmental conditions such as ionizing radiation and desiccation.[15] The orange carotenoid protein is employed by cyanobacteria to activate photoprotection in high-light conditions.[16] The selection is based on the diverse chromophores and photoactivation mechanisms of these photoreceptors. Nevertheless, owing to their ability to perceive and respond to light stimuli, photoreceptors have garnered significant interest not only in understanding natural biological processes but also in pioneering applications in the realms of optogenetics and biological imaging.[17–19]

The review is organized in accordance with the general workflow outlined in Figure 1. This workflow initiates with characterization of the dark state, encompassing both structural and spectroscopic aspects. It then proceeds to investigate the photochemical process through (non) adiabatic dynamics simulations. Finally, it simulates the system's transition to the active state using molecular dynamics and enhanced sampling techniques. Prior to delving into the workflow's details, we provide a brief introduction to the three selected photoreceptors and we highlight the aspects of their functionality that remain to be fully comprehended.

Three different photoreceptors and their still unanswered questions

Some photoreceptor families contain small flavin-binding domains that exert the photosensing function. These are the Light, Oxygen and Voltage (LOV), cryptochromes (CRYs) and **Blue Light-Using Flavin (BLUF)** domains.[2,3,20] All of them are water-soluble proteins that bind a flavin, either as flavin adenine dinucleotide (FAD) or flavin mononucleotide (FMN), but have completely different activation mechanisms. For example, in LOV domains, absorption of blue light triggers the formation of an adduct between FMN and the conserved active-site Cys, in a mechanism that occurs via triplet states. Adduct formation is accompanied by a shift in the flavin absorption band from 447 nm to 490 nm.

BLUF domains do not show such drastic chemical and spectroscopic changes upon photoactivation, which has complicated the investigation of the activation mechanism. However, consistent spectroscopic changes are observed among BLUF photoreceptors, such as a $\sim$10 nm red shift of the flavin absorption spectrum and a $\sim$20 cm^{-1} downshift in the infrared (IR) frequency of the C4=O carbonyl stretching.[21] Essential for BLUF photoactivation are the strictly conserved Tyr21 and Gln63 residues located close to the isoalloxazine ring of flavin.[2] It was suggested that changes in hydrogen bonding within the flavin binding pocket

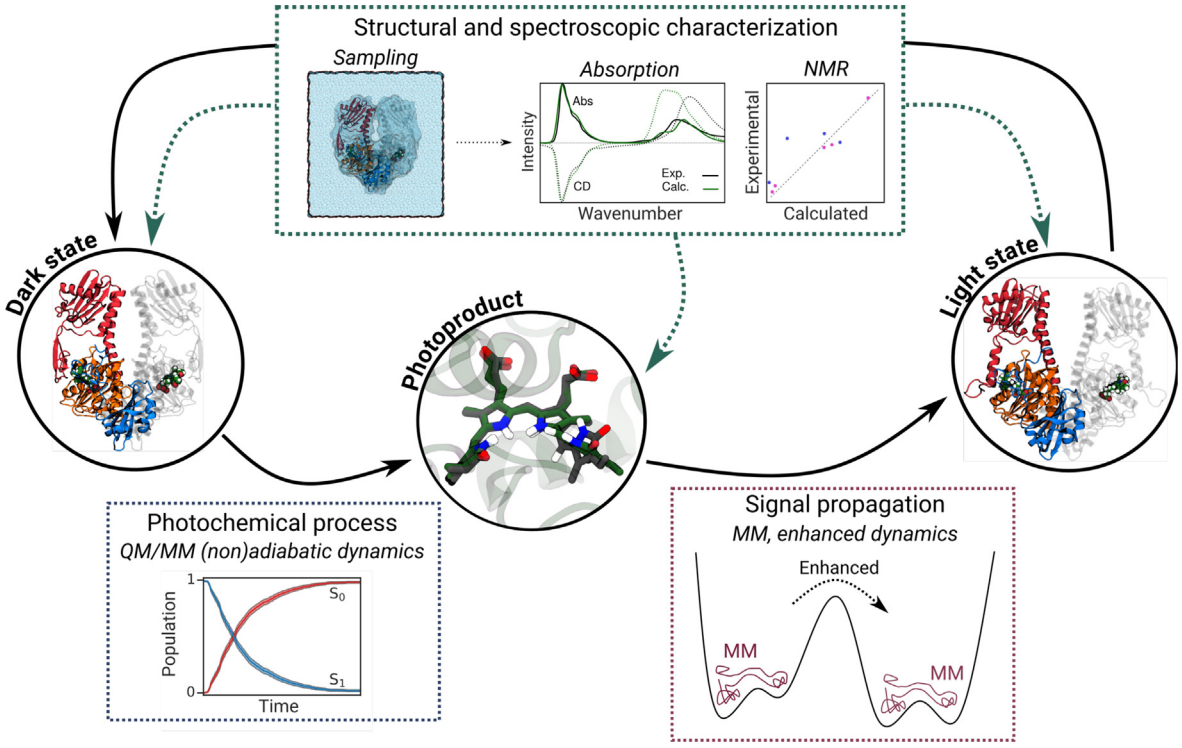

Fig. 1. General workflow for modeling the photoactivation of photoreceptors. First, it is necessary to obtain the structure of the dark state from experiments (or computational predictions) (see Section 'Structural characterization'). Here, the dark state of the *Deinococcus radiodurans* bacteriophytochrome (DrBph) is represented as an example. Afterward, we can sample the configurational space of the solvated photoreceptor through μs-long MM MDs. The validation of the sampling is then performed with a spectroscopic characterization by comparing calculated and experimental spectra (UV–vis, circular dichroism, IR, NMR, *etc.*) (see Section 'The simulation of spectroscopic signatures'). Subsequently, after a refinement of the PES of the QM subsystem achieved with ps-long QM/MM MDs, it is possible to investigate the photochemical process with QM/MM (non) adiabatic techniques (see Section 'The photochemical event'). Finally, to investigate the further evolution towards the active state (here, the active state of DrBph) it is possible to apply enhanced sampling techniques in combination with MM force fields (see Section 'Signal propagation'). The same techniques employed for the dark state can be used to characterize the photoproduct and light state.

could be responsible for the observed spectroscopic changes. A further complication in the interpretation of BLUF mechanism came from the conflicting structures first resolved for the BLUF domain of the AppA protein (AppA-BLUF) present in the purple bacterium *Rhodobacter sphaeroides*.[22,23] Similarly, two different structures were resolved for the BLUF domain of the *Synechocystis* Slr1694 photoreceptor.[24] These structures differ in the presence of either a Trp or a Met in the active site (Trp_{in} and Met_{in} respectively), and in the orientation of Gln63. The coexistence of such structures led researchers to propose a Trp-to-Met substitution as a part of the photoactivation mechanism.[24,22] Another proposed mechanism instead involved the tautomerization of the active site Gln63.[25,23]

The AppA protein was among the first flavoproteins containing BLUF domains to be discovered.[14] In addition to the BLUF domain, it contains a C-terminal SCHIC (sensor containing heme instead of cobalamin) domain that senses redox conditions. The biological mechanism of AppA was demonstrated *in vitro* and *in vivo*: in the dark or in low-light conditions, AppA binds to the transcriptional repressor PpsR, inhibiting the binding of PpsR to DNA; upon blue-light absorption, AppA is activated and dissociates from PpsR, which can bind to DNA and inhibit the transcription of photosynthetic genes.[14,21] Notably, most spectroscopic and structural investigations were performed on truncated constructs containing only the BLUF domain of AppA. However, a more complete structural model for the dark-state AppA was more recently obtained, along with a structure of the AppA-PpsR complex.[26]

Phytochromes are a large family of photoreceptors found in plants, bacteria, and fungi.[27,15] They are red-absorbing homodimeric proteins, where each monomer is composed of a generally conserved photosensory module (PSM), composed of three domains PAS (Per/Arndt/Sim), GAF (cGMP phosphodiesterase/adenyl cyclase/

FhlA), and PHY (Phytochrome specific), and a photoswitchable bilin (a linear tetrapyrrole) chromophore covalently anchored to the protein via a cysteine residue. In all known phytochromes, the chromophore is embedded inside the GAF domain. Its chemical structure can change depending on the organism: phytochromobilin (PΦB) is the molecule responsible for light absorption in plant phytochromes; whilst the phytochromes from bacteria and cyanobacteria bind biliverdin IXα (BV) and phycocyanobilin (PCB), respectively. A hallmark feature of phytochromes is that they can adopt two spectroscopically different photoreversible forms: the red light-absorbing form, also known as Pr state, and the far-red light-absorbing form, the Pfr state, which differs by both chromophore stereochemistry and protein structure. The resting state of "canonical" phytochromes is the Pr state. However, a number of bacteriophytochromes, known as bathy phytochromes, show reversed stability, with the Pfr being the thermodynamically stable state. This different behavior is not due to the chromophore but instead to the specific composition and shape of the binding pocket.[28,29] When exposed to red light, the chromophore is electronically excited and photoisomerizes at the double bond between C- and D-rings (Figure 4). Afterwards, the chromophore structural change propagates first to the binding pocket, and then downstream to the PAS, GAF, and PHY domains.[30–32] The "reverse" light-to-dark reaction can occur via a thermal pathway or by absorption of a second photon of far-red light. Even if the structures of the active and inactive states have been characterized and we know the main features of the initial photochemical event at the embedded bilin chromophore, many aspects of the photoactivation mechanism are still unknown. Experimental data indicate that the process involves intermediates with varying lifetimes, from nanoseconds to milliseconds, but their transitions, quantity, and molecular details are still unclear. Additionally, we lack insight into how the initial photoinduced change spreads from the chromophore's binding pocket to the entire protein and how protein residues impact the stability of metastable states.

The presence of crystallized active and dark states for the *Deinococcus radiodurans* bacteriophytochrome allowed the investigation of the role of conserved amino acids of the binding pocket using site-directed mutagenesis.[33] The Pr form is relatively unaffected by individual mutations. This is because the bright excitation (*Q* band) of phytochromes originates primarily from a chromophore-localized $\pi \rightarrow \pi^*$ transition.[34] The only effect on the spectral properties of Pr is a change in the absorption ratio of the Soret/*Q* band. Some mutations, on the other hand, are deleterious to the complete photoconversion: substitution of His290 with Gln and several substitutions of Asp207 block photoconversion from Pr to Pfr at the Meta-R intermediate or even earlier.[33]

Orange Carotenoid Protein (OCP) is a small water-soluble protein responsible for activating photoprotection in cyanobacteria by photoconverting from the inactive orange form (OCP^O) to the active red form (OCP^R), which interacts with the cyanobacterial phycobilisome causing its quenching, as demonstrated both *in vivo* and *in vitro*.[16,35] OCP naturally binds a ketocarotenoid, such as echinenone (ECN) 3'-hydroxyechinenone, or canthaxhanthin (CAN), in a pocket formed between its two domains, the N-terminal domain (NTD) and C-terminal domain (CTD). This structure is kept together by two H-bonds between conserved Tyr201/Trp288 and the carotenoid's carbonyl group.[35–37] Upon photoactivation, these H-bonds are broken and the carotenoid translocates into the NTD,[37] causing the separation between the two domains. However, the exact structure of OCP^R was not known[35] until very recently, when the structure of a quenched phycobilisome was resolved by cryo-electron microscopy.[38] While time-resolved spectroscopy experiments have provided insights into several intermediates in the photoactivation process,[39] the complete understanding of OCP's photocycle remains elusive. However, the primary enigma surrounding OCP centers on the initial photochemical event. This challenge arises from the intricate dynamics of carotenoid excited states and the exceptionally low quantum yield of photoactivation, making direct spectroscopic evaluation of the process difficult. Various hypotheses have been proposed to elucidate the excited-state dynamics of the carotenoid bound to OCP and to clarify how photochemistry disrupts the hydrogen bonds with the protein.

Characterization of the inactive/active states

In this Section, we will discuss the computational strategies that can be used to characterize the structure of photoreceptors in their inactive or resting state. This can be considered as a preliminary step, necessary to gain confidence in the resting-state structural ensemble prior to simulating the activation mechanism. However, most of the considerations made in this Section also apply to the characterization and validation of the active (signaling) state, and of any intermediate states.

Structural characterization

Frequently, the crystallographic structure of the inactive and the active states of photoreceptors cannot be established with certainty. In general, X-ray structures can deviate from the solution structures as a consequence of crystal packing artifacts.[40] Moreover, the relatively short lifetime of the signaling states hinders their structural characterization with experimental methods, and modified

conditions are needed to obtain a structure for the signaling states. Multiple experimental sources should then be taken into account to determine the structure of photoreceptors, particularly in the signaling state.

The first step for the characterization of photoreceptors is the determination of a structural ensemble representative of the one in solution. We mention here that several photoreceptors can exist in solution as dimers or oligomers. For example, phytochromes are proteins that naturally exist in a dimeric state, and their functionality is reliant on this specific dimeric structure.[41] BLUF domains also tend to form dimers or larger structures.[42,43] The OCP from Synechocystis is known to crystallize as a dimer and is likely present in a dimeric form in solution.[44] In all of these instances, it is unlikely that the dimerization significantly impacts the structure of the active site or the optical properties of the chromophores. Therefore, the characterization of the protein may be made considering only one monomer. Nevertheless, it is crucial to examine this aspect, as the dimeric form of photoreceptors may be essential for signal transduction.

The most basic approximation would be to refine the crystal structure, focusing especially on the chromophore-binding pocket using QM/MM methods (see below). This approach is based on the strong assumption that a single crystal structure is representative of the conformational ensemble of the photoreceptor, which may be true only for a quite rigid pocket. On the other hand, having a single structure would greatly simplify the analysis of spectroscopic signals and the comparison with experiments. Unfortunately, the intricate and dynamic network of interactions that generally characterize the binding pocket makes this approximation not reliable. Additionally, this method fails to consider the influence of an external solvent, which can be particularly significant when the embedded chromophore is exposed, affecting the energetics of the photoprocess.

The most general and reliable approach to investigate the solvated photoreceptor is to use classical molecular dynamics (MD) simulations based on Molecular Mechanics (MM) force fields. MD allows simulating the photoreceptor in the natural solution environment, possibly relaxing the crystal artifacts. In addition, MM-MD can in principle sample the entire conformational ensemble of the photoreceptor, thus enabling the description of structural and spectroscopic heterogeneity. However, it is very challenging to accurately characterize the conformational space of the selected state for complex systems such as photoreceptors. Two main limitations hinder the description of conformational ensembles through MD simulations.

A first limitation is the quality of the MM force field, which has to accurately describe not only the potential energy of the protein and solvent, but also that of the chromophore. General force fields for small organic molecules are usually employed for protein cofactors, and do not require derivation of parameters. However, chromophores are conjugated molecules, and their description through a standard MM force field is not at all straightforward. Tuning or re-derivation of parameters through comparison with QM data may be therefore needed to obtain a realistic description of the chromophore in MD simulations. Another solution would be to supplement the MM-MD sampling with QM/MM simulations. These simulations are orders of magnitude more expensive, and therefore limited to short times, but can be used to validate or correct the ensembles obtained from MM-MD.

A second limitation is related to the extent of sampling of the conformational space that can be achieved by MD simulations. The time scales realistically achievable by standard MD simulations vary depending on the size of the system. For photoreceptors, microsecond simulation times are now routinely attained. Assuming that the conformational motions of the photoreceptor are faster than the μs scale, such simulations can provide a realistic sampling of the resting state. To control the extent of MD sampling and reproducibility of the results, it is important to run several independent replicas of the same simulation. Different random sampling of initial velocities in the MD will ensure that different results are obtained from each replica. Convergence of the MD sampling within a conformational state is achieved if all replicas give the same distribution of the observables of interest. In practice, this condition is never attained in MD simulations of such complex systems, but the variability among replicas provides a confidence interval on the results.

If the conformational dynamics of the resting state is slower than the timescales that can be simulated with plain MD, one can resort to enhanced sampling techniques. As these methods are especially useful for simulating the changes upon photoactivation, we will discuss such techniques in the Section ‘Exploring longer timescales’.

As an example of the use of MD simulations, we describe here the characterization of the BLUF domain of the AppA protein (AppA-BLUF) for which two contrasting structures were found,[22,23] suggesting that different experimental conditions influence the obtained structure. The two structures differ in the geometry and composition of the active site (Figure 2).[22,23] The structure by Anderson et al. features a Trp in the flavin binding pocket, making a hydrogen bond with the amide oxygen of the conserved Gln.[22] On the other hand the structure by Jung et al. [23] has a Met in the active site, and the

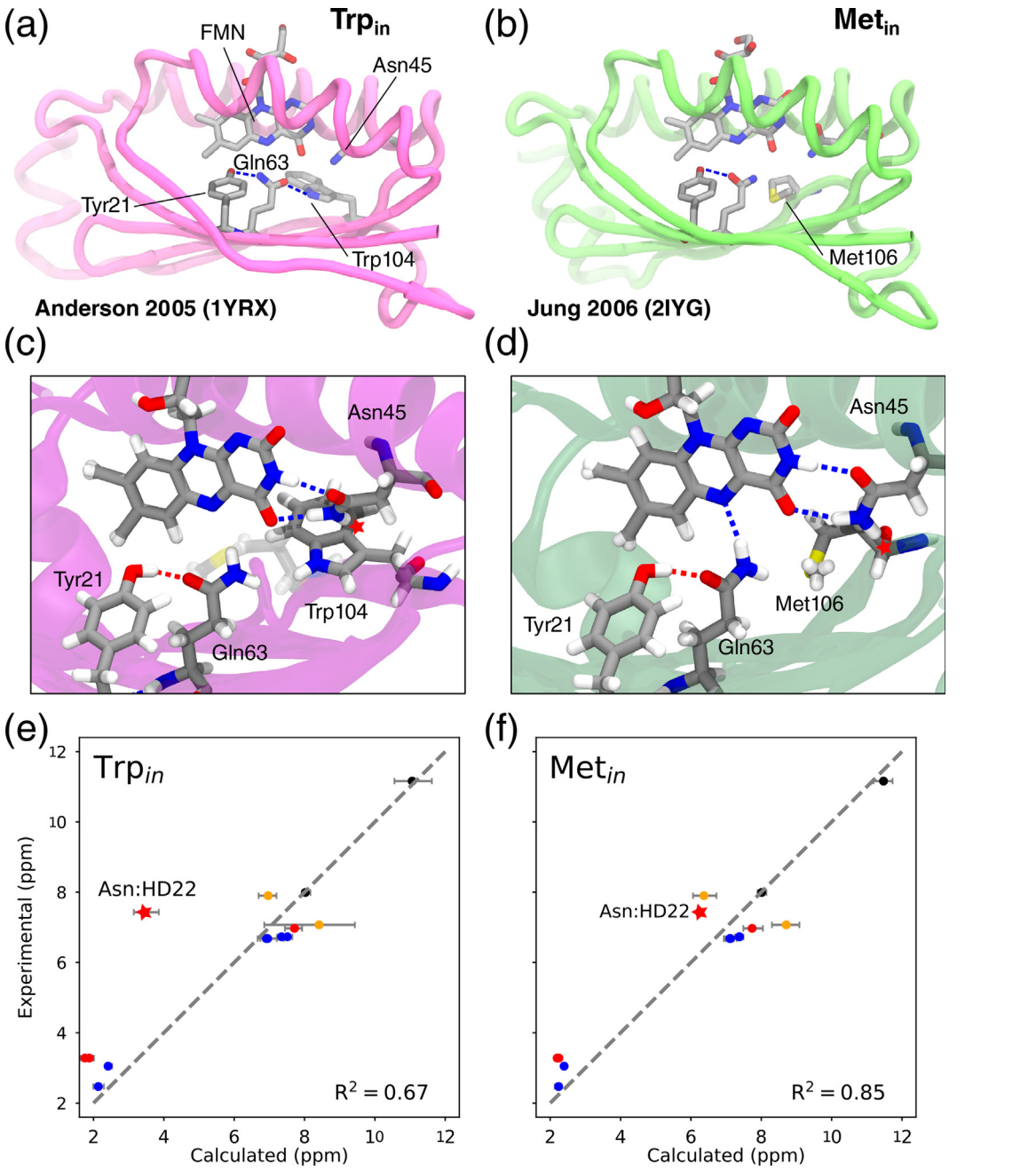

Fig. 2. Structure and NMR spectroscopy of AppA-BLUF. (a,b) Crystal structures of AppA-BLUF. (a) Trp_{in} structure by Anderson et al. (PDB 1YRX)[22]; (b) Met_{in} structure by Jung et al. (PDB 2IYG).[23] The active-site residues and the FMN cofactor are represented as bonds. (c,d) Representative structures of the active site of the (c) Trp_{in} and (d) Met_{in} structures obtained from the MD simulations of Ref.[45] (see text). The HD22 proton of Asn45 is highlighted with a red star. (e,f) Comparison between the calculated and experimental[43] chemical shifts for (e) Trp_{in} and (f) Met_{in} structures. The HD22 proton of Asn45 is highlighted with a red star. Panels (e,f) are adapted from Ref.[45]

Gln shows the opposite orientation. Crucially, the orientation of the Gln amide group could not be directly determined by the X-ray map at the resolution of the experiments, but it was deduced on the basis of hydrogen bonds with the neighboring residues.[22] Finally, a structural ensemble deduced from NMR distance restraints suggested yet another organization of the active site.[43]

MD simulations on the two structures were performed by several research groups, with contradicting results.[46–48] Some groups observed a rotation of the key Gln residue starting from the Anderson structure, with no preferential orientation

adopted, while for others the initial Gln orientation remained stable. Later, some of us performed μs MD simulations and observed a rotation of the Gln side chain.[45] Interestingly, the Gln initially experiences very fast interconversion between the two orientations, and stabilizes only after hundreds of ns in the same orientation as found in the Jung structure. This observation can be explained by the presence of a hidden conformational variable that slowly relaxes from the crystal structure towards the free-energy minimum sampled in the MDs. Thus, the Gln side chain experiences a time-dependent potential that initially allows the Anderson-like orientation of Gln, but eventually stabilizes the opposite orientation (Figure 2). The MD simulations also unequivocally show that Gln rotation in AppA-BLUF is a fast motion, and easily adapts to the conformation of the rest of the protein. On the other hand, the position of the residue (Trp or Met) inside the binding pocket of either structure remains stable in the MD simulations, suggesting that both conformations represent at least metastable states. This example clearly demonstrates the need of μs-scale MD simulations for characterizing the structure of photoreceptors. In fact, only in this time scale it becomes clear which motions are slow, and thus determine distinct states in the photoreceptor's conformational landscape. Furthermore, such long simulations allow excluding unrealistic structures (such as the Anderson X-ray structure) from consideration when simulating spectroscopic signatures.

The simulation of spectroscopic signatures

Spectroscopy simulations and the comparison with experiments can provide a way to validate the structure of the resting or active state. Spectroscopic evidence can reveal information on the active site or sometimes on farther regions of the protein. The presence of a chromophore in the active site naturally suggests the use of electronic spectroscopy, such as UV/Vis absorption, to probe the geometry of the chromophore and its environment. However, vibrational (IR or Raman) and NMR spectroscopy can also be used to obtain structural information on either the resting state or the changes upon photoactivation.

Before discussing how to simulate the various spectroscopies, it is worth mentioning that simulating the spectroscopic signals of photoreceptors requires taking into account the effect of the environment (protein residues, cofactors, and water) on the region of interest, even if the chromophoric moiety is localized on a small region. This is usually done with QM/MM methods (See the Section 'Multiscale quantum/classical approaches'). It is also important to note that quantum mechanical calculations introduce some errors on the calculated signals, in addition to the errors arising from structural discrepancies. These errors are intrinsic of the quantum mechanical method or of the QM/MM embedding approximation, and should be kept in mind when comparing with experiments. In most cases, it is more useful to compare trends between different structures, such as resting and signaling states, rather than absolute values.

Spectroscopy simulations can be used in different ways to help characterize the structure of photoreceptors. First, they can be used to support or refute a structural model for the resting state or for the active state individually.

One interesting case of spectroscopic validation of a structure is that of AppA-BLUF, as there are two conflicting structures for the resting state (see the Section 'Three different photoreceptors and their still unanswered questions').[22,23] Several groups have attempted to use UV/Vis spectra calculations to substantiate one of the two structures, but the difference in excitation energy between the two structures is too small to draw meaningful conclusions.[46,49,45] Colette et al. compared absorption spectra in a different way: they employed an electrostatic model to predict the effect of mutations on the flavin absorption spectrum, which allowed them to pinpoint the structure from Jung et al. as the most likely candidate for the resting state.[50]

NMR experiments allowed assigning chemical shifts to most protons in the AppA-BLUF active site.[43] As these chemical shifts report on the local environment of the flavin and neighboring residues, they represent another means of validating the resting-state structure. This led Hashem et al. to calculate and compare the proton chemical shifts of the two contradicting structures with the experiment.[45] To do so, they employed the solution structures obtained after microsecond MD relaxation, which display the same orientation of Gln63 but have different residues in the active site (see above). They focused on the residues surrounding the flavin, as they are key conserved active-site residues. While both structures showed a reasonable agreement between calculated and measured chemical shifts, the Anderson structure showed a worse agreement for some protons (Figure 2). In particular, the amide proton of Asn45 was dramatically shielded in this structure. The effect could be traced back to the position of Trp104 inside the binding pocket, whose shielding cone is oriented towards the Asn45 sidechain. This strongly indicates that the Trp position is incompatible with the assigned chemical shifts. Along with the other pieces of evidence, the spectroscopic validation allowed a confident determination of the resting-state structure of AppA-BLUF.

A more refined but more complicated spectroscopic validation is the calculation of spectroscopic differences between resting and active states. These include spectroscopic shifts in vibrational or electronic transition frequencies, or even absorption difference spectroscopies such as difference IR. One advantage of such a

strategy is that systematic errors due to the quantum chemical methodology largely cancel when considering differences between two structures. Furthermore, a comparison of the predicted differences with the experimental ones can give information on both inactive and active states. However, the results require a more careful interpretation, as any discrepancy with experiments may be attributed to errors in either the resting or the active-state structure.

Photoreceptors usually show different absorption spectra in the resting and signaling states. Computing the spectral differences can not only help validate the structures of these states, but also allow understanding which factors determine the spectral shifts. Such an approach was used by Macaluso et al. when comparing the absorption lineshapes for Pr and Pfr states of the DrBph phytochrome.[51,34] They computed the absorption and circular dichroism spectra for the two states, including vibronic and inhomogeneous effects in the lineshape. The calculations reproduced quite well the differences observed upon photoactivation for both the absorption bands considered. Although the overall absorption shift between Pr and Pfr can be explained simply by the isomerization of the chromophore, other aspects such as the relative intensity of the CD bands and the overall lineshape could be only reproduced by considering the entire MD ensemble of the Pfr state. Analyzing the heterogeneity of the Pfr excitation energies, it was concluded that spectroscopically distinct conformations occur in the binding pocket of the Pfr state.

Similar calculations were performed by Bondanza et al. on OCP.[52] They compared the inactive state OCP^O with the N-terminal domain (NTD) of OCP, also called red carotenoid protein (RCP), which is spectroscopically similar to the active state OCP^R. By considering again vibronic and inhomogeneous effects in the absorption lineshape, they could reproduce both the red shift and the band broadening observed passing from OCP^O to RCP.

A more complex case is represented by infrared spectroscopy. Although IR gives a wealth of information on the chemical identity and environment of the probed system, a direct measurement of the resting or signaling state would be useless, because the entire holoprotein contributes to the observed spectrum. Experimentally, IR difference spectroscopy is used to capture only the change in IR absorbance upon photoactivation, even in a time-resolved manner.[53] Negative and positive bands in an IR difference spectrum correspond to signals in the inactive and active states, respectively. If a clear experimental assignment is available, for example through isotopic substitutions, one can extract the vibrational frequency shifts that occur upon photoactivation, and compare them with calculations. For example, the experimental shifts in the flavin C4 = O stretching frequency observed upon photoactivation of AppA-BLUF were used by Khrenova et al. to validate their proposed mechanism of photoactivation.[54]

When there is strong heterogeneity in vibrational frequencies, or the assignment of all peaks is not clear from the experiments, it is possible to directly simulate the IR difference spectra, by simply subtracting the calculated spectra of active and inactive states. In the spirit of QM/MM methods, one can focus on the IR difference signals that arise from the chromophore in order to investigate the changes occurring in the active site, assuming that such signals are well separated. Macaluso et al. calculated the IR difference spectrum of the BV chromophore within the DrBph phytochrome, limited to the frequency window where the BV carbonyls absorb.[51] The good agreement with experiments[55] allowed substantiating the hydrogen bond network around the D- and A- rings of the BV.

Simulation of IR spectroscopy was useful also to assign the peaks of AppA-BLUF experimental spectra. Macaluso et al.[56] exploited a combination of classical MM MD and Born–Oppenheimer QM/MM MD simulations (see Section 'Born-Oppenheimer dynamics') on both ground and excited state, to compute IR spectra of both states, and to reproduce the experimental transient IR spectrum.[57] With this strategy, they were able to characterize the isoalloxazine ring region of the spectrum and to identify ultrafast structural changes in the protein-embedded chromophore following excitation.

The role of specific amino acids in the spectroscopy of photoreceptors can be experimentally assessed by site-directed mutagenesis. For example, the frequency shift upon mutation of a specific residue can give insight into the electronic structure of the chromophore as well as on the position or protonation of that amino acid side chain. Mutation effects can be investigated also computationally. Within a MD strategy, this requires repeating MD simulations and QM/MM calculations for each mutated system. This is needed to capture the mutation effects on the structure of the active site and the effect of changing the electrostatics of the surroundings on the chromophore's spectroscopy. A simplification can be done by assuming that the structure of the system does not change significantly upon mutation, and the only relevant effect is the electrostatic interaction between the chromophore and the mutated residue. Using an electrostatic model in place of QM/MM calculations further simplifies this problem and allows an effective screening of mutation effects.[50]

Multiscale quantum/classical approaches

An effective strategy to simulate the spectroscopy of photoreceptors is introducing a hybrid quantum

mechanics/molecular mechanics (QM/MM) model.[58,59] In these approaches, the chromophore, possibly together with some strongly interacting residues or solvent molecules, is treated using a QM method, while the protein and the rest of the environment are described with a classical MM force field. This ensures that the highly heterogeneous surroundings are accounted for in the electronic description of the active site.

The QM/MM strategy can be formulated in various ways by using a different definition of the QM-MM coupling. In the most common version of the model, the coupling between the QM and MM subsystems is described using the electrostatic embedding scheme, whereby the QM subsystem is directly perturbed by the point charges which represent the MM atoms as defined by the specific force field.

An alternative and more complete formulation involves the incorporation of QM–MM mutual polarization effects, achieved through the introduction of a polarizable force field. By including their flexible polarizable nature, these force fields can offer a system-specific, relaxed electrostatic picture. This becomes particularly crucial when dealing with molecules embedded in proteins, where specific interactions and local charge imbalances are common. Indeed, in regions with a high concentration of charged amino acids, describing them solely in terms of fixed charges may lead to the emergence of a strongly localized charged region. Such a scenario can lead to an artificially high polarization of the QM subsystem, most likely resulting in an inaccurate or even qualitatively incorrect description. In a polarizable embedding QM/MM approach, instead, the polarization can counteract the electric field produced by the point charges, yielding a more realistic representation of the electrostatic effects exerted by the protein.

Different formulations are now available for polarizable embedding QM/MM and they differentiate in terms of the way polarization is represented.[60,61] The most popular models are those using fluctuating charges[62–66], Drude oscillators[67,68], or induced point dipoles (IPD). [69–78,61]

QM/MM approaches also differ for the flavor of QM method employed. There is no single technique appropriate for the system or problem of interest, as the applicability range of a method also depends on the process one wants to describe and on the complexity of the electronic structure of the chromophore.

To simulate vibrational or NMR spectroscopies, ground-state density functional theory (DFT) methods generally represent the most effective approach in terms of accuracy and computational cost. Among wavefunction theory approaches, we mention the second-order Møller-Plesset perturbation theory (MP2), which can be more accurate and is still affordable for large systems.

When moving to electronic spectroscopies, and more in general the simulation of excited states and the related photophysics and photochemistry, things become much more complicated. Single-reference excited-state methods describe the excitations from a single-reference ground-state wave function.[79] These methods include the popular time-dependent DFT (TD-DFT) together with more advanced wavefunction methods such as algebraic-diagrammatic construction (ADC) and coupled cluster (CC) methods.[80] As these methods make quite strong assumptions on the nature of the ground state, their application is limited to the cases where the ground state is well separated from all the excited states. This is usually the case when a chromophore is in its ground-state geometry, therefore these methods are generally employed for the calculation of excitation energies and absorption spectra. The unrivaled popularity of TD-DFT methods is certainly connected with their simplicity and reduced computational cost. Importantly, TD-DFT methods do not describe well certain classes of excitations, such as charge-transfer (CT) states, although specific density functionals have been designed to mitigate this problem, and extensive benchmarks are available. We only mention here that long-range corrected (LC) functionals are mandatory for describing systems that have charge-transfer excitations, as only these functionals guarantee a correct asymptotic behavior of electron–hole separations.[79]

A much less expensive alternative is given by semiempirical methods, which combine a simplified molecular orbital description and empirical parameters.[81] Semiempirical methods based on the modified neglect of diatomic differential overlap have been used extensively also for photochemistry.[82] The more recent family of orthogonalization-corrected methods (OM1, OM2, OM3) showed improved accuracy for both ground and excited states.[83] Another class of semiempirical methods, based on DFT is density functional tight binding (DFTB) with its TD extension for excited states.[84]

More recently, there has been an increased interest in excited-state SCF methods, normally referred to as ΔSCF.[85–88] In ΔSCF, the excited state is described as a single determinant, in the same way as the ground state. This leads to a broken-symmetry solution for excited states, which nonetheless appears to be effective in treating CT states or double excitations, where TD-DFT methods seem to fail. The ΔSCF description is less flexible than TD-DFT, but works well when the excited state of interest is well described by a single configuration.

Multireference methods are needed whenever there is strong electron correlation, that is, when even the ground state is a superposition of multiple electronic configurations.[89] Such methods become mandatory when ground and excited states

become close in energy. Among the ab initio multireference methods, we mention in particular the complete-active-space SCF (CASSCF), where the wavefunction includes all possible configurations within an active space of orbitals. This method takes into account strong correlation, but accounting for dynamic correlation is fundamental to obtain reasonable excitation energies. The most common way to include the remaining electron correlation is to use second-order perturbation theory such as in the CASPT2 method. Multireference methods are fundamental to correctly describe the electronic structure when ground and excited states are close in energy, which is often the case for photochemical events, but also for systems with a complex electronic structure such as carotenoids.

The photochemical event

From a modellistic point of view, photochemical reactions can be investigated using two different strategies, a static and a dynamic one. The main difference between static and dynamic approaches lies in the fact that static approaches focus on the electronic properties of the system at fixed geometries, while dynamic approaches explicitly account for the molecular motion and evolution during the photochemical reaction.

In the next two sections, we will delineate the two strategies separately, highlighting their respective strengths and limitations. Nevertheless, it is essential to emphasize that researchers frequently employ a combination of static and dynamic methods to achieve a comprehensive understanding of photochemistry in molecules.

Regardless of the chosen approach, photoreceptors invariably involve a chromophore inserted in a highly anisotropic binding pocket through a complex network of covalent and noncovalent interactions with protein residues. As a result, the protein exerts a significant influence on the photoreaction pathways, leading to the opening or inhibition of certain relaxation channels that may not be accessible in the isolated molecule. Hence, incorporating the protein and the external environment in the simulations is essential to capture the actual behavior of the system. To account for environment effects, both static and dynamic strategies commonly exploit the QM/MM methods described in the Section 'Multiscale quantum/classical approaches'.

The static strategy

The static characterization of light-induced reactions in molecules generally starts from the exploration of potential energy surfaces (PESs) of the relevant electronic states, using an appropriate QM method. Typically, the computational exploration of the PESs begins with the determination of the ground-state minimum geometries and the calculation of the excited state energies at the optimized minima, i.e. Franck–Condon (FC) points. Next, the PESs for the lowest excited states are characterized by computing the molecular geometries of minimum and conical intersection (CoIn) points. The determination of CoIn, i.e. molecular geometries where two (or more) adiabatic electronic states are degenerate, is particularly important because they represent funnels for efficient radiationless transition between states. In addition, relaxed scans, or linear interpolations, along different internal coordinates of the chromophore are generally performed to determine photochemical reaction pathways.

As mentioned in the Section 'Multiscale quantum/classical approaches', multireference methods represent the strategy of choice for photochemistry, although these methods are generally very computationally expensive. One of the most common strategies is to use CASSCF to optimize the molecular geometries of minimum and CoIn points, and then compute CASPT2 energies as single-point calculations on the CASSCF optimized structures. In this way, dynamic electron correlation effects, largely missing in CASSCF, are recovered by CASPT2 at an affordable computational cost. This approach, often referred to as CASPT2//CASSCF, has been used to compute photochemical reaction pathways in different photoresponsive proteins, such as rhodopsins [90–96], LOV proteins,[97] phytochromes[98] and the photoactive yellow protein.[99,100]

For large chromophores, such as tetrapyrroles in phytochromes and or carotenoids in OCP, ab initio multi-reference QM methods are computationally very demanding or even unfeasible. In fact, accurate CASSCF calculations on large π-electron systems may require orbital active spaces exceeding the current computational limit. In these situations, more approximate QM methodologies have to be employed. Among them, single-reference methods such as second-order coupled cluster (CC2) and TD-DFT represent cost-effective approaches. As explained above, these methods generally fail to describe the PESs close to CoIn with the ground state, while they are often suitable to compute the excited states in the vicinity of the FC region. For phytochromes, the TD-DFT method was used to compute excited-state relaxed scans along different torsion angles of the bilin chromophore.[101–103] In addition, CC2 calculations were performed to elucidate the photochemical behaviour of the photoactive yellow protein chromophore.[104,105] Much less expensive methods to compute excited states are semiempirical configuration interaction techniques, such as OM2/MRCI. The latter has been recently employed to explore the low-lying PESs of the keto-carotenoid canthax-

anthin in OCP.[106] The successful comparison with ab initio multireference calculations also suggested that these semiempirical methods may be a suitable alternative to single-reference methods, as they can still provide a multireference description of the electronic structure.

An alternative strategy to reduce the computational cost is to truncate the chromophore and perform accurate calculations on smaller model systems. This approach was used to study a phytochrome chromophore model by means of relaxed scans in the excited state using the CASPT2//CASSCF method.[107] More recently, energy profiles for several phytochrome chromophore models were determined by performing geometry optimizations, as well as linear interpolations of internal coordinates, at the CASPT2 level.[108] We remark that this is a risky strategy, as truncating the conjugation of a chromophore may drastically alter its properties.

Static approaches are useful for understanding the potential energy surfaces of different electronic states and identifying key stationary points (e.g., ground-state minima, excited-state minima, and transition states). However, as they do not capture the dynamic behavior of the molecular system during photochemical reactions, they can only give a qualitative indication of the main photochemical pathways that can occur in the photoreceptor. A more detailed and realistic representation of the photochemical process is instead caught by dynamic approaches. They can reveal the pathways and mechanisms of photochemical reactions, including non-adiabatic transitions and energy dissipation.

The dynamic strategy

Simulating the light-induced dynamics in molecular systems generally calls for a proper description of transitions between different electronic PESs, called nonadiabatic transitions where the adiabatic, or Born–Oppenheimer (BO), approximation breaks down. This situation typically occurs at crossings or CoIn points, and calls for the consideration of couplings between different PESs. Nonetheless, there are systems where BO simulations [109,52,78,110] can provide valuable insights into the mechanism of interest. In such cases, the trajectory is propagated in an adiabatic manner along a specific excited state.

Here below we describe first the strategies for "simplified" BO dynamics, and then explain the most common nonadiabatic dynamics methods used for photoreceptors.

Born–Oppenheimer dynamics. Born–Oppenheimer excited-state dynamics can be useful to investigate qualitatively the evolution of the chromophore in the excited state, or even to gain more information on its photochemistry. Its applicability however depends strongly on the system of interest. In some cases, BO dynamics has to be integrated with assumptions on what happens when a crossing between potential energy surfaces is encountered. Such quasi-BO simulations have proven useful in describing Proton-Coupled Electron Transfer (PCET) mechanisms in BLUF photoreceptors.[111–113] This process involves not only the pigment (the flavin) but also two close-by protein residues, a tyrosine and a glutamine.[25] The photochemistry proceeds by a photoinduced electron transfer from the conserved tyrosine to the flavin chromophore, coupled with a double proton transfer.[25] A key step of the mechanism though is the behavior of the system after the electron transfer has taken place, that is, when the system is in a charge transfer state. This means that following one excited state is enough to understand some characteristics of the photochemistry.

The above-mentioned mechanism starts with blue-light absorption, and the flavin is excited to its lowest $\pi_{\text{flavin}} \rightarrow \pi^*_{\text{flavin}}$ excited state (locally excited, LE state). After few ps, protein reorganization drives an electron transfer from tyrosine to the excited flavin generating a charge-transfer (CT) state formed by a negatively charged flavin and a positively charged tyrosine. Because of this charge separation, the system transfers protons to compensate for the charge imbalance: a first proton is transferred from the tyrosine to the glutamine, and a second one from the glutamine to the flavin. As a result both the tyrosine and the flavin are neutralized and a singlet diradical ground state is obtained (Forward PCET, Figure 3a). Then, the system undergoes the rotation of the imidic acid group, forming a new network of hydrogen bonds (Gln rotation, Figure 3a). The last step consists of another PCET process, in which a back electron transfer occurs from flavin to tyrosine, followed by a double proton transfer from flavin to Gln and from Gln to Tyr, reaching the light-adapted state (Reverse PCET, Figure 3a).

This mechanism was studied using BO excited-state dynamics in two different systems (AppA-BLUF and Slr1694-BLUF), and with different QM/MM methods.[111–113] In both cases the classical, atomistic representation of the surrounding environment was fundamental to obtain realistic dynamics. However, Goings et al.[111] employed an electrostatic embedding QM/MM method, while Mazzeo et al.[113] used polarizable embedding. In both cases, the QM part included both Tyr21 and Gln63 as they are actively involved in the reaction. The TD-DFT and ΔSCF methods were used to propagate the initial excited-state dynamics, which led to different results due to their inherent methodological differences (See Section 'Multiscale quantum/classical approaches').

TD-DFT molecular dynamics simulations were used in both Refs. [111,113] to observe the excited-

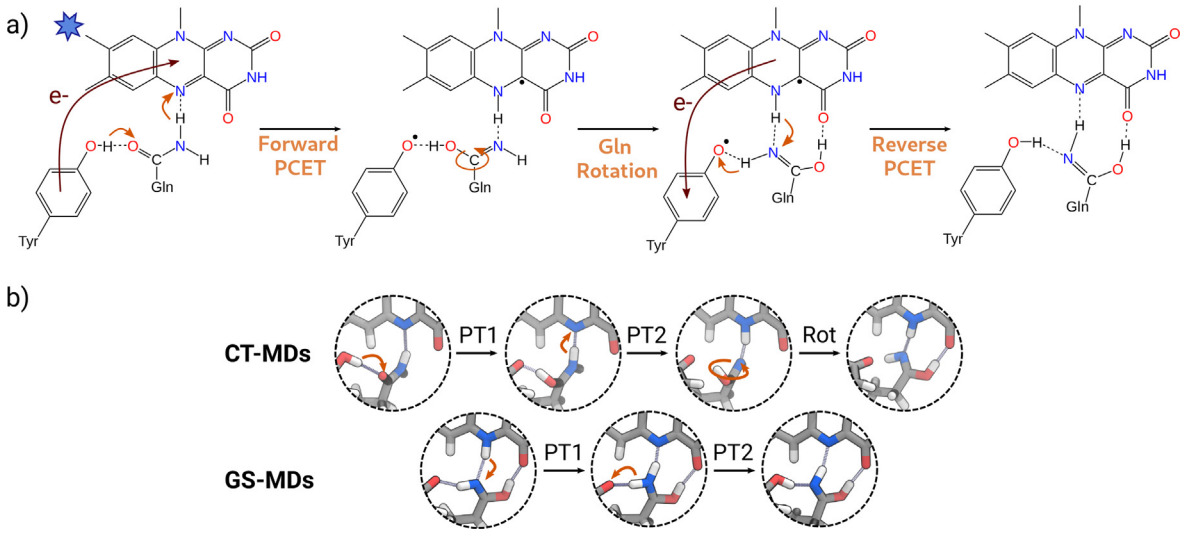

Fig. 3. (a) One of the proposed mechanism of activation of BLUF proteins.[25] (b) Snapshots of the ΔSCF (CT-MDs) and DFT (GS-MDs) trajectories performed on AppA-BLUF. All figures are adapted from Ref.[113]

state evolution upon photoexcitation. In TD-DFT simulations, a specific excited state is selected, and the trajectory is then propagated adiabatically along this chosen excited state. In this case, the nature of the excited state evolves smoothly (i.e., adiabatically) following the nuclear motion. In BLUF domains the first excited state (S_1) is initially populated, as it corresponds to the spectroscopically accessible LE state.[111] As the simulation progresses, due to the effects of the protein, the energy of the CT configuration becomes lower than that of the LE state. Consequently, S_1 changes smoothly from a LE to a CT character, indicating the occurrence of electron transfer.[111] Such a transition can be detected by a sharp change in the dipole moment of the excited state or by a rapid decrease of the transition dipole moment. Immediately after the transition to the CT state, a first proton transfer is observed from Tyr21 to Gln63.[111,113] The second proton transfer was observed only by Goings et al. in their TD-DFT simulations.[111]

The general agreement between the two simulations on different systems supports both the electron transfer and the following double proton transfer. However, we must note that the BO approach relies on the unphysical assumption that the LE → CT transition occurs with 100% probability whenever the two states cross, in an adiabatic fashion. The small energy gaps at LE → CT transitions instead suggest that nonadiabatic effects are substantial.[111] This issue also limits the possibility to directly compare PCET timescales with experiments. In fact, the charge separation timescales (∼1 ps) predicted by this approach are much faster than the experimental ones (tens of ps).[7,114]

As the sequential double proton transfer leads to a neutral ground state with a diradical character, TDDFT cannot be used anymore, since it is not suitable to describe the multiconfigurational nature of the state. For this reason, Goings et al.[111] switched to spin-flip TD-DFT for their excited-state simulations. This methodology exploits a high spin reference determinant in conjunction with a $\alpha \rightarrow \beta$ spin-flip operator to include the ground state as the lowest excited state. In this way, also ground states with a multireference character can be described.

As an alternative method, Mazzeo et al. employed ΔSCF to propagate the excited-state dynamics. Because of its nature, ΔSCF can describe excited states as a single configuration; hence, it lacks the capability to observe the LE → CT transitions.[113] As a result, with ΔSCF one can follow a specific (quasi) diabatic state. For this reason, the ΔSCF simulations are not strictly Born–Oppenheimer, and they do not describe adiabatic transitions at all. On the other hand, they allow following the diradical open-shell state formed through electron transfer all the way to its equilibrium. The ΔSCF simulations started in the CT state described the double proton-transfer and the subsequent rotation of the imidic acid residue (CT-MDs, Figure 3b).

The back electron transfer involved in the last step of the mechanism (reverse PCET) was simulated by manually moving an electron from flavin to tyrosine: starting from the final structures of spin-flip TDA and ΔSCF simulations for Slr1694-BLUF and AppA-BLUF, respectively, the trajectories have been propagated on the closed-shell determinant, using restricted DFT.[113,112] This closed-shell state is higher in energy than the diradical system, because of the charge-separation (positively charged protonated flavin and a negatively charged deprotonated tyrosine). Proton transfers that annihilate the charge separation and lead to

the light state are shown in the snapshots of GS-MDs, Figure 3b.

From this example, it becomes clear that BO excited-state dynamics require several assumptions on the photochemical pathways, and can be useful to verify a mechanism, rather than for an unbiased exploration of the excited-state dynamics. Furthermore, the simulations performed on the PCET mechanism of AppA do not provide predictions on the kinetics of charge separation or recombination. In principle, the nonadiabatic dynamics methods described in the next Section could be used to simulate the entire excited-state dynamics of the system. However, the charge separation/recombination steps occur at longer time scales (at least 60 ps),[114] which prevents a direct simulation of their dynamics. In such a context, the BO simulations still allow for a mechanistic interpretation of the photochemistry, at the price of requiring precise assumptions on the charge transfer steps.

Nonadiabatic dynamics. Several different approaches can be used to simulate the nonadiabatic dynamics of molecular systems, ranging from fully quantum dynamics, where both electrons and nuclei are treated quantum mechanically, to semiclassical methods, where the nuclear motion is described classically.[82,116–118]

The most commonly used technique to simulate the light-induced nonadiabatic dynamics in photoreceptor chromophores is the semiclassical surface hopping (SH) method. In SH, an ensemble of independent classical trajectories is used to approximate the quantum nonadiabatic dynamics of molecular systems. In each trajectory, the nuclei move, according to classical mechanics, on one electronic PES at a time (referred to as the "active" PES) and transition probabilities between electronic states are computed to decide whether the trajectory will continue evolving on the "active" PES or hop to another one.

Among the different SH variants,[118] Tully's "fewest switches" surface hopping (FSSH)[119] represents the most widely used SH scheme. The FSSH method requires the coupled propagation in time of both the nuclear and electronic motion and nonadiabatic transitions between states are taken into account, at each time step of the trajectory, according to a stochastic algorithm based on the computed transition probabilities.[119] The popularity of FSSH is mainly due to its good compromise between computational efficiency and accuracy of results, especially for medium-sized and large systems. However, FSSH suffers from an improper account for quantum decoherence effects and for this reason an appropriate decoherence correction scheme needs to be included in the simulations.[120,121]

Due to the stochastic nature of the FSSH algorithm, a large number of SH trajectories (typically a few hundred) needs to be computed to achieve statistical convergence of the results and to observe rare reactive events. This can significantly increase the computational cost, especially when the PESs are computed along the trajectories using ab initio QM methods such as CASSCF. For this reason, a simplified SH algorithm, called diabatic SH, was proposed. In this method, a nonadiabatic transition is allowed only when the trajectory crosses the CoIn hyper-line between two states.[122] Although this way of restricting hops could lead to an incorrect determination of the state lifetimes, it allows identifying the main relaxation pathways involving CoIn points, using only a few trajectories (i.e. $\leqslant$50).

FSSH was widely employed, in combination with the CASSCF method, to simulate the photo-induced dynamics in different rhodopsins.[123,124,92,125,126] More recently, FSSH simulations with semiempirical PESs were performed to investigate the nonadiabatic excited-state dynamics in a channelrhodopsin,[127] in a phytochrome[115] and in OCP.[128] The diabatic SH was used to simulate the light-induced dynamics in the photoactive yellow protein[122,129] and, more recently, in a bacteriophytochrome.[130]

One more rigorous approach to simulate the nonadiabatic molecular dynamics is the ab initio multiple spawning (AIMS) technique developed by Martínez and co-workers.[131] In this method, the nuclear quantum dynamics in the excited states is described using a set of multi-dimensional Gaussian functions, called trajectory basis functions (TBF), moving classically on the different electronic PESs. When a TBF reaches a region of strong coupling, a nonadiabatic transition is described using a spawning procedure whereby a new TBF is created on the coupled electronic state. Since each TBF follows its own classical trajectory and the population transfer between TBFs traveling on different PESs is treated quantum mechanically, the AIMS method allows for a more accurate description of decoherence effects, compared to SH, without the need for ad hoc corrections. However, the computational cost of AIMS is generally larger than SH and increases quadratically with the number of TBFs (N_{TBF}). For this reason, AIMS simulations can become computationally too demanding when many nonadiabatic transitions occur during the excited-state dynamics leading to a large increase of N_{TBF}. In the field of photoreceptors, the AIMS method has been employed to investigate the light-induced nonadiabatic dynamics in rhodopsins,[132–135] as well as in the chromophores of the photoactive yellow protein and the green fluorescent protein.[136–139]

All these simulations have clearly shown that the protein does not act as a rigid matrix but plays a fundamental role in determining the photochemical mechanism and its energetics.

An example of the control exerted by the protein on the excited-state dynamics of the embedded chromophore has been recently shown by some of us[128] for OCP. As already mentioned in Section 2, the photochemical event initiating the photoactivation of OCP is still under debate. The reported spectroscopic investigations have shown that a complex excited-state dynamics is involved where multiple dark electronic states with different lifetimes play a role. Specifically, in addition to the typical S_1 ($2A_g^-$) state of carotenoids, a faster decay is generally attributed to an intramolecular charge transfer (ICT) state, strongly coupled with S_1, while a slower decay is associated with a dark S^* state.[39] By using QM/MM SH nonadiabatic dynamics simulations we revealed that while the $S_1 \rightarrow S_0$ excited-state decay of CAN exhibits a single-exponential behavior in the gas phase, in OCP, the S_1 population decay follows a multi-exponential pattern, consistent with spectroscopic observations. These variations in S_1 lifetimes stem from the ground-state structural heterogeneity of the carotenoid within OCP and in particular they are associated with the puckering conformation of the end ring of CAN which is hydrogen-bonded to the CTD (β_1 ring). We also showed that the S^* state can be explained with a specific puckering conformation of the β_1 ring of CAN. Moreover, we found a minor $S_1 \rightarrow S_0$ decay pathway involving the isomerization of a double bond of CAN adjacent to the β_1 ring in the CTD, an event not observed in the gas phase simulations. This pathway has been closely linked to the rapid-decaying S_1/ICT sub-population, leading us to suggest that this photoisomerization serves as the catalyst for OCP photoactivation.

Another example of the protein control on the initial photochemical process is that found in phytochromes. As described in Section 2, the bilin chromophores embedded in phytochromes upon absorption of red light, photoisomerization around a double bond. In a recent work,[115] we have used QM/MM SH nonadiabatic dynamics to investigate the molecular mechanism of this photoisomerization in the *Deinococcus radiodurans* bacteriophytochrome.

The many interactions established between the protein residues in the binding pocket and BV induce a counterclockwise rotation of the double bond that links the terminal D ring to the rest of the molecule (Figure 4). Simultaneously, the neighboring single bond rotates in the opposite direction. This coordinated motion, often referred to as the "hula-twist" in the literature, facilitates isomerization around the double bond without causing significant alterations to the molecule's three-dimensional structure.[9,140,141] Such a mechanism, previously proposed for other conjugated systems including photoactive proteins,[122,128,142,143] has been confirmed in another study, using a different QM description and a different approach for simulating the excited-state dynamics.[130] The structural heterogeneity of the chromophore[144] is also reflected in the excited state lifetimes. The nonadiabatic dynamics simulations have shown that the rate of the photoisomerization is strongly determined by a hydrogen bond between the D-ring carbonyl group of BV and a nearby histidine residue and that the non-radiative decay from S_1 to S_0 proceeds through a CoIn. It is interesting to note that the presence of this H-bond does not enhance the photoprocess but instead it slows it down, which shows that its role is mostly to stabilize the inactive state to ensure a thermal reversion in the dark. Upon reaching the CoIn region, the hydrogen bond is lost because of the constraints imposed by the CoIn geometry, and the reaction can proceed even if with a low quantum yield.

Signal propagation

The local changes in the active site induced by the photochemical event propagate through the entire protein, leading to large-scale motions that activate the photoreceptor, and finally trigger its biological function. Typically, these processes involve several intermediate states that are reached in different time scales, from picoseconds to milliseconds and beyond. In principle, the sequence of intermediates and the mechanisms leading from one to the other are not known. Therefore, in order to reach an atomistic view of photoreceptors' photoactivation, it may be necessary to combine a range of different computational techniques able to access different time scales.

To provide an overview of these techniques, we first describe the strategies to simulate the events that immediately follow the photochemistry, on timescales faster than the microsecond. Then we will outline the methods that can be used to investigate processes that occur on longer time scales.

After the photoproduct

When the chromophore is back to the ground state, it is possible to simulate the subsequent dynamics with ground-state QM/MM molecular dynamics. This allows not only to characterize the primary photoproduct but also to simulate its spectroscopic properties, which can be used to validate the results of the simulations with experiments. In this validation, the same techniques used for the characterization of dark/light state described in Section 'Structural characterization' can be used.

A limited time window can be explored by QM/MM dynamics: few picoseconds with an ab initio QM method or few nanoseconds with semiempirical methods. To widen this window while keeping the computational costs affordable, one can switch to fully MM MD simulations. These simulations can

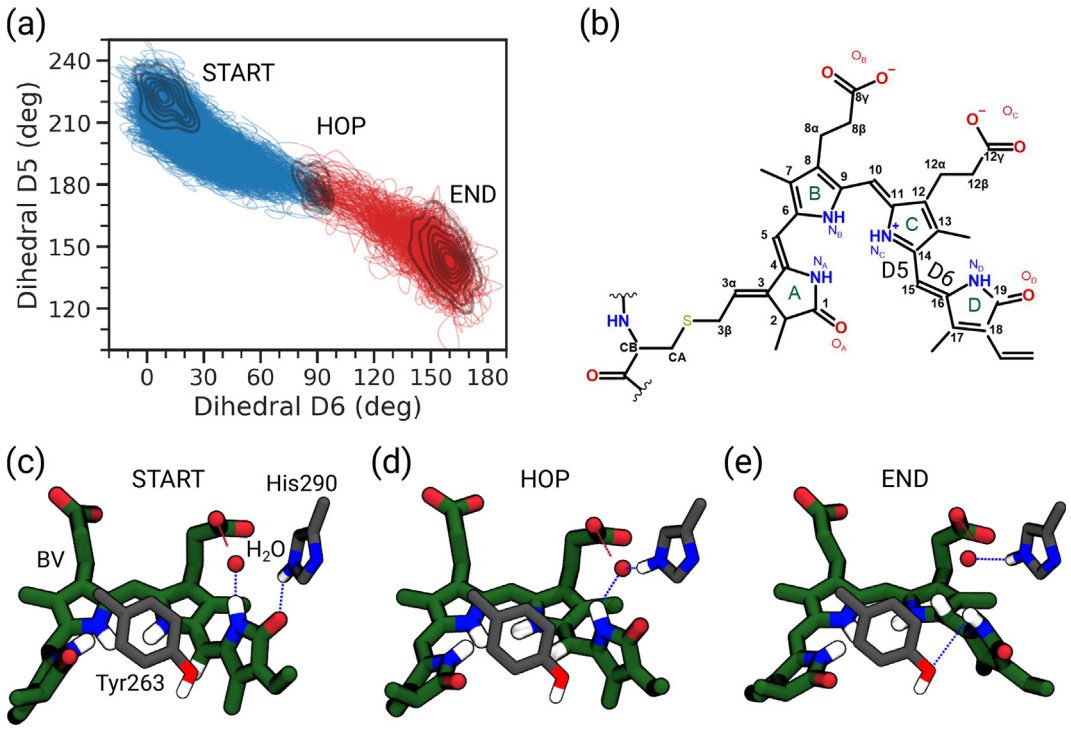

Fig. 4. Photoisomerization of BV in the bacteriophytochrome. (a) Correlation between the dihedral angles D5 and D6. All reactive trajectories are shown using blue lines for those running on S_1, and red lines for those on S_0. The density distribution is shown at the starting conditions, at the $S_1 \rightarrow S_0$ transition, and at the end of the simulation. (b) BV chemical structure and definition of the main dihedral angles involved in the photoisomerization. (c), (d), (e) Representative structures of the chromophore at the beginning of the simulation, at the time of the $S_1 \rightarrow S_0$ transition, and at the end of the simulation. The main hydrogen bonds involving the D-ring are highlighted. All panels are extracted from Ref.[115]

explore up to timescales of the order of microseconds.

Some of us used this protocol to follow the evolution of the photoproduct obtained by SH nonadiabatic dynamics.[115] With ground state QM/MM trajectories on the nanosecond time scale, we observed an evolution of the photoproduct towards an intermediate stabilized by a hydrogen bond of the amide proton of BV's D ring with a tyrosine residue. Such an intermediate was characterized by calculating its IR spectroscopic features which were finally compared with transient IR spectra showing a good agreement in reproducing the Pr-to-intermediate change in both the position and shape of the CO_D signals. Starting from the intermediate, a swarm of MM MD trajectories, in the μs timescale, was generated. This investigation showed the evolution of the early intermediate into a late intermediate in a timescale compatible with the experiment,[55] featuring a more disordered binding pocket and a weakening of an arginine-to-aspartate salt-bridge interaction, whose cleavage is essential for phytochrome activation.

Also in the case of AppA-BLUF, Hashem et al.,[145] investigated the evolution of the final product of the double PCET process by using MM MD simulations in the microsecond timescale. The simulation showed that the change in the BLUF domain upon photoactivation is rather local and mainly induced by small differences in the binding mode of flavin in the active site. The altered H-bond pattern causes the flavin to move in a slightly different position within the binding pocket. In turn, this induces a change in the conformation of an arginine residue, located in a different region of the binding pocket, which reflects on its interaction with farther residues. These predicted structural changes were finally validated by IR, NMR, and UV–vis spectroscopic characterizations.

Exploring longer timescales

In order to simulate the larger conformational changes of the protein, which usually occur on longer than microsecond timescales, it is necessary to employ methods that accelerate the exploration of the conformational space. These techniques, known as enhanced sampling methods, were developed to either explore the conformational space of biomolecules or even to obtain realistic estimates of free energy differences and barriers between metastable states. Before describing these methods, it is worth noting that photoactivation mechanisms are

inherently nonequilibrium events with a preferential free energy gradient created by the initial photochemistry. The application of such accelerated techniques, while sometimes unavoidable, should be taken with a grain of salt, given that these methods are meant to provide the best possible characterization of the equilibrium distribution of a system.

The idea behind every enhanced sampling method is to modify the dynamics of a system by introducing a bias, allowing for faster exploration of the potential energy landscape. The interested reader is referred to the more specialized reviews providing a more detailed overview of enhanced sampling methods.[146–151]

In the enhanced sampling approach, the bias potential can be applied along an "effective" reaction coordinate, in which case it falls under the so-called collective variable (CV)-based methods. The CV is a function of atomic coordinates that describe specific aspects of the system's behavior (dihedral, distance, angle, RMSD, and so on). A good CV must be able to distinguish not only all the relevant metastable states but also the transition states between them. The design of the required CV(s) is not trivial, often requiring extensive prior knowledge. Popular collective variable-based methods are umbrella sampling (US),[152] Metadynamics and related methods,[153,154,146] among which we cite well-tempered metadynamics (wt-MetaD) and variationally enhanced sampling (VES).[155] In metadynamics and related methods, a time-dependent bias is added depending on the history of the system. The bias is constructed so as to discourage the regions of the CV that were already visited in the simulation, enhancing the exploration of the configurational space. Assuming that the simulations have converged, such methods also allow a quantitative determination of the free-energy profile along the CV.

If the CV is optimal, CV-based methods are extremely efficient in exploring the potential energy surface. However, in complex environments such as photoreceptors, because of the many chromophore-protein interactions that are established as the system evolves, converging the simulations is extremely difficult, meaning that the system will explore different configurations, but no information can be obtained on their relative stability. A necessary condition for convergence is that multiple transitions are observed between the different states of the system throughout the simulation.

The VES method was used to sample nonequilibrium configurations of the bilin chromophore in both the Pr (dark) and Pfr (light) forms of DrBph phytochrome.[156] The authors circumvented photochemistry by using two collective variables: the double bond that connects the D-ring to the rest of the chromophore and the adjacent single bond. While with an isolated chromophore the simulation achieves convergence very quickly, when the protein is introduced, achieving the same result becomes much more complex because the phytochrome protein pocket is densely packed with residues.

In these situations, convergence can be sped up by incorporating environment-aware variables. In practice, the number of CVs is limited to a maximum of three due to the prohibitive scaling of the computational cost with the dimensionality. To deal with that, path-based methods such as the nudged elastic band[157] and adaptive biasing potential optimization (ABPO)[158] have been devised. They require some knowledge of the initial and final states and possibly an initial guess path. The ABPO method was successfully used to propose the exchange between Trp and Met in the active site of the Slr1694 and AppA BLUF domains.[159,160] CVs can be directly defined so as to describe the progress along a predefined path, and then used with a CV-based method like Metadynamics. These path CV methods[161,162] have the key advantage that the bias is now added along a one-dimensional progress coordinate. Recently, path CVs have been used to deliver free-energy profiles for the deactivation of two BLUF proteins, BlrB and AppA.[163] The authors, by employing this approach, corroborated a proposed mechanism based on the rotation and tautomerization of a conserved glutamine.

Other methods apply more general biases, and can be referred to as unconstrained methods.[151,150,164] Among the most popular, we mention the "tempering" methods, which are based on the fact that the sampling is much easier and faster at higher temperatures than at lower temperatures. The most widely used tempering-based enhanced sampling is parallel tempering (PT) or temperature replica exchange (REMD).[165,166] Here, several replicas at different temperatures are performed simultaneously. At a certain simulation time, an exchange between a pair of replicas with neighboring temperatures is done with an acceptance probability that depends on the potential energy difference between the two replicas. For an effective PT simulation, the potential energy fluctuations of such replicas need to have an appreciable overlap. Therefore, for large systems many replicas are needed, making PT simulations rather costly.

Although these methods are more computationally demanding than a CV-based approach, they usually require less *a priori* information. As a result, they can be used if data on neither the final state nor a potential collective variable are available to obtain useful information about the metastable states and the reaction mechanism. REMD simulations of the LOV protein Vivid were able to reproduce key conformational changes associated with the light activation process that are observed experimentally.[167]

Replica exchange methods can also be combined with CV-based methods to reduce the quality requirements of the CVs as the unconstrained method will help sample the orthogonal degrees of freedom not included in the CV set.

As an example of combining different enhanced sampling methods, we describe the investigation of the photoactivation of OCP (Figure 5). Contrary to the cases mentioned above, the identity of the primary photoproduct in OCP photoactivation is still unclear (see above). Bondanza et al.[168] focused directly on identifying the intermediates encountered upon translocation of the carotenoid into the NTD and dissociation of the domains. To effectively simulate the translocation, they combined a CV-based method, umbrella sampling (US), with the REMD unconstrained method. They identified as a CV the distance between the carotenoid and the

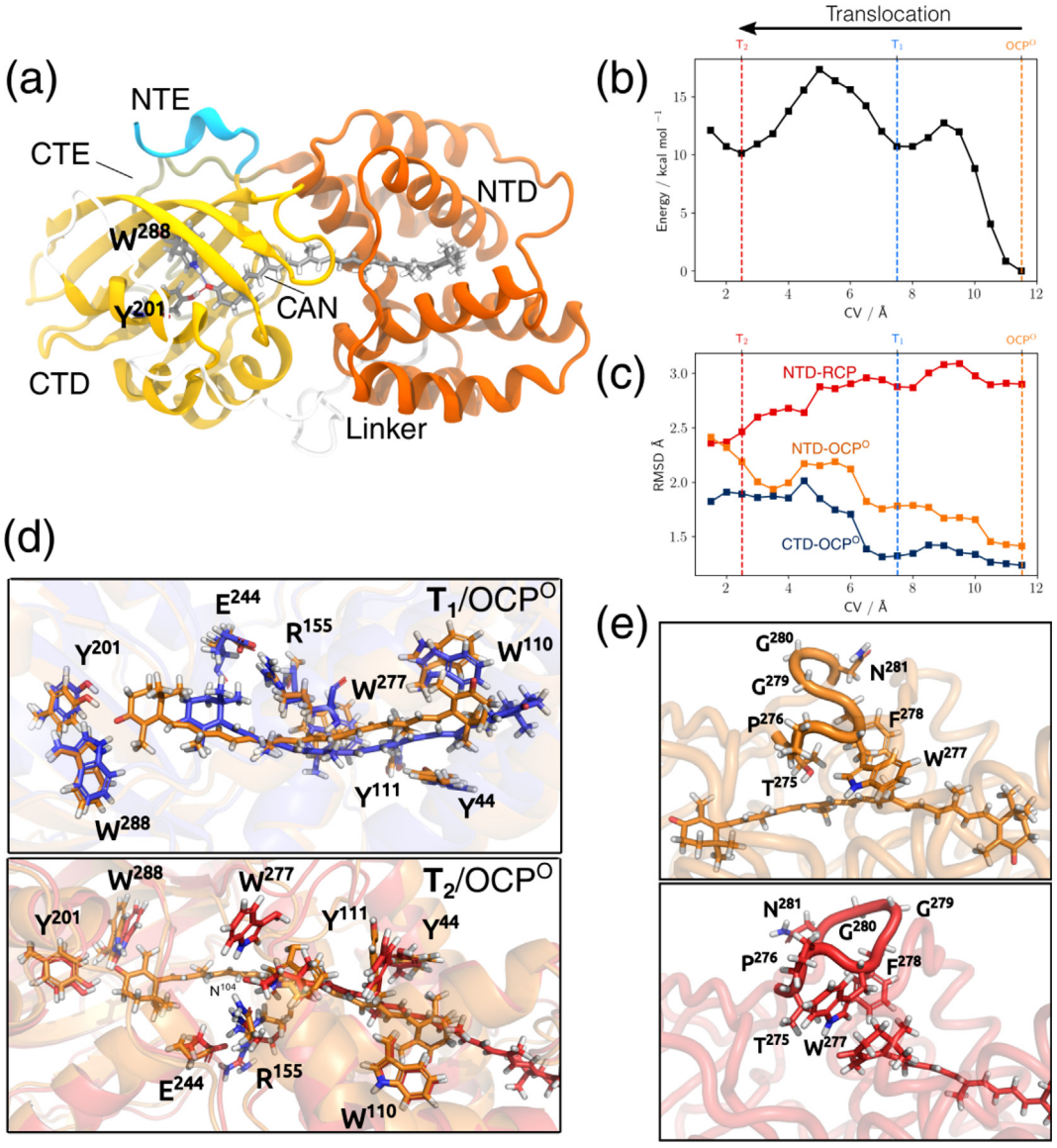

Fig. 5. Translocation of the carotenoid in OCP via a combination of umbrella sampling and REMD. (a) Structure of OCP^O. Different domains are shown with different colors, the C-terminal extension (CTE) is in brown and the N-terminal extension (NTE) is in cyan. The cantaxanthin (CAN) carotenoid is also shown with H-bonds to Tyr201 and Trp288. (b) Free-energy profile as a function of the distance between the CAN and the NTD; the translocation occurs in the opposite direction indicated by the arrow. The free-energy minima corresponding to OCP^O and the intermediates $\mathbf{T}_1$/$\mathbf{T}_2$ are indicated with the vertical lines. (c) RMSD of the domains with respect to OCP^O (dark blue and orange lines) or RCP[37] (red line). (d) Carotenoid binding pocket in the $\mathbf{T}_1$ (top, blue) and $\mathbf{T}_2$ (bottom, red) intermediates, compared to OCP^O (orange). (e) Conformational change in the loop 275–281 of the CTD upon carotenoid translocation. Representative structures in OCP^O (top, orange) and $\mathbf{T}_2$ (bottom, red). Panels (b-e) are taken from Ref. [168] (CC-BY).

NTD center, which is expected to approximately describe the motion of the carotenoid. At the same time, REMD allowed exploring all the remaining degrees of freedom, such as the rearrangement of the protein to accommodate the carotenoid.

This US-REMD combination allowed obtaining accurate estimates of the free-energy profile along the translocation coordinate (Figure 5b) and corresponding intermediates (Figure 5d), which were identified with the spectroscopic intermediates obtained by time-resolved IR.[39] The last intermediate is characterized by a fully translocated carotenoid and a structure of the NTD similar to the RCP,[37] which demonstrates the ability of the method to correctly predict the changes in the protein structure. Key residues that rearrange during the translocation were also identified, including the entire 275–281 loop in the CTD (Figure 5e), and their role in stabilizing the intermediates was elucidated. Finally, the availability of the translocated intermediate allowed simulating the dissociation of OCP using well-tempered metadynamics. Although these simulations did not achieve a quantitative determination of the dissociation free energy landscape, they clearly indicated that translocation of the carotenoid is needed for domain dissociation.[168] This study demonstrates that profound atomistic insight can be obtained with a careful combination of enhanced sampling techniques, but at the same time highlights the cost of obtaining quantitative thermodynamic or kinetic information on the photoactivation path.

Conclusions and perspectives

Modeling photoreceptors at the atomic level presents a formidable challenge. However, recent advancements in both theoretical models and computational tools have significantly enhanced our ability to gain a deeper understanding of their functioning. As we have shown in this review, these developments have shed light on the critical role that the protein plays in governing the molecular mechanisms, as well as in regulating the energetics and kinetics. Hand-in–hand with experimental investigations, computational approaches have helped unveil the atomistic details of photoactivation for a diverse set of photoreceptors.

Notwithstanding the successes of computational approaches, significant limitations persist, hindering broader and more effective application of this approach. The primary constraint lies in the complexity of the strategy, which calls for an intricate combination of diverse methods. This complexity prevents a uniform exploration of the entire photoactivated process, with a particular challenge in describing the propagation of structural changes from the chromophore to the protein. As shown in this review, this propagation encompasses numerous time scales, making it impossible to adopt a single dynamic approach. Instead, excited-state (nonadiabatic) QM/MM dynamics and full MM (enhanced) dynamics must be artificially linked at a certain point, albeit at the risk of potentially overlooking specific steps, or introducing artifacts. The solution to this problem is neither easy nor straightforward. One promising avenue towards achieving this objective is the use of machine learning (ML) strategies. In the last years, artificial intelligence and ML have revolutionized protein structure prediction especially thanks to AlphaFold and its successor AlphaFold2.[169,170] However, in recent times, ML-based interatomic potentials have also emerged as a viable alternative to traditional QM and MM methods for predicting potential energies and forces.[171–173] This approach has also been extended to encompass electronic excited states, offering an effective means for conducting (non) adiabatic dynamics simulations.[174,175] The substantial reduction in computational cost achievable with this ML-based approach could enable tracking the light-induced structural changes within the embedded pigment, extending beyond the photoproduct to encompass the subsequent evolution in the ground state, including the formation of intermediates.

The emergence of exascale computing can bring about a significant revolution in the realm of scientific simulations, both for classical[177] and ab initio [176] molecular dynamics. The power of exascale machines can be only fully exploited by massively parallel algorithms. For example, stochastic simulations such as surface hopping will become much easier with exascale computing power, as hundreds of simulations can be run independently at the same time. Furthermore, if ML techniques become routine, the parallel computing power of exascale machines can be harnessed to train very large ML models in reasonable time.

DECLARATION OF COMPETING INTEREST

The authors declare that they have no known competing financial interests or personal relationships that could have appeared to influence the work reported in this paper.

Acknowledgments

D.A, L.C. and B.M acknowledge funding by the European Research Council, under the Grant ERC-AdG 786714 (LIFETimeS).

Received 13 September 2023;
Accepted 2 November 2023;
Available online 7 November 2023

Keywords:
photochemistry;
nonadiabatic dynamics;
QM/MM;
molecular dynamics;
enhanced sampling techniques

References

[1]. van der Horst, M.A., Hellingwerf, K.J., (2004). Photoreceptor proteins, star actors of modern times: a review of the functional dynamics in the structure of representative members of six different photoreceptor families. *Acc. Chem. Res.* **37**, 13–20.
[2]. Losi, A., (2007). Flavin-based blue-light photosensors: a photobiophysics update. *Photochem. Photobiol.* **83**, 1283–1300.
[3]. Conrad, K.S., Manahan, C.C., Crane, B.R., (2014). Photochemistry of flavoprotein light sensors. *Nat. Chem. Biol.* **10**, 801–809.
[4]. Burgie, E.S., Vierstra, R.D., (2014). Phytochromes: an atomic perspective on photoactivation and signaling. *Plant Cell* **26**, 4568–4583.
[5]. Kottke, T., Xie, A., Larsen, D.S., Hoff, W.D., (2018). Photoreceptors take charge: emerging principles for light sensing. *Annu. Rev. Biophys.* **47**, 1–23.
[6]. Möglich, A., Yang, X., Ayers, R.A., Moffat, K., (2010). Structure and function of plant photoreceptors. *Annu. Rev. Plant Biol.* **61**, 21–47.
[7]. Kennis, J.T.M., Mathes, T., (2013). Molecular eyes: proteins that transform light into biological information. *Interface Focus* **3**, 20130005.
[8]. Brunk, E., Rothlisberger, U., (2015). Mixed quantum mechanical/molecular mechanical molecular dynamics simulations of biological systems in ground and electronically excited states. *Chem. Rev.* **115**, 6217–6263.
[9]. Gozem, S., Luk, H.L., Schapiro, I., Olivucci, M., (2017). Theory and simulation of the ultrafast double-bond isomerization of biological chromophores. *Chem. Rev.* **117**, 13502–13565.
[10]. Andruniów, T., Olivucci, M., (2021). QM/MM Studies of Light-responsive Biological Systems. Springer Nature.
[11]. Mroginski, M.-A. et al, (2021). Frontiers in multiscale modeling of photoreceptor proteins. *Photochem. Photobiol.* **97**, 243–269.
[12]. Weik, M., Domratcheva, T., (2022). Insight into the structural dynamics of light sensitive proteins from time-resolved crystallography and quantum chemical calculations. *Curr. Opin. Struct. Biol.* **77**, 102496.
[13]. Nottoli, M., Cupellini, L., Lipparini, F., Granucci, G., Mennucci, B., (2021). Multiscale models for light-driven processes. *Annu. Rev. Phys. Chem.* **72**, 489–513.
[14]. Masuda, S., Bauer, C.E., (2002). AppA is a blue light photoreceptor that antirepresses photosynthesis gene expression in rhodobacter sphaeroides. *Cell* **110**, 613–623.
[15]. Takala, H., Edlund, P., Ihalainen, J.A., Westenhoff, S., (2020). Tips and turns of bacteriophytochrome photoactivation. *Photochem. Photobiol. Sci.* **19**, 1488–1510.
[16]. Kirilovsky, D., Kerfeld, C.A., (2016). Cyanobacterial photoprotection by the orange carotenoid protein. *Nat. Plants* **2**, 16180.
[17]. Christie, J.M., Gawthorne, J., Young, G., Fraser, N.J., Roe, A.J., (2012). LOV to BLUF: flavoprotein contributions to the optogenetic toolkit. *Mol. Plant.* **5**, 533–544.
[18]. Mathes, T., Kennis, J.T.M., (2016). Editorial: optogenetic tools in the molecular spotlight. *Front. Mol. Biosci.* **3**
[19]. Nemukhin, A.V., Grigorenko, B.L., Khrenova, M.G., I. Krylov, A., (2019). Computational challenges in modeling of representative bioimaging proteins: Gfp-like proteins, flavoproteins, and phytochromes. *J. Phys. Chem. B* **123**, 6133–6149.
[20]. Lukacs, A., Tonge, P.J., Meech, S.R., (2022). Photophysics of the blue light using flavin domain. *Acc. Chem. Res.* **55**, 402–414.
[21]. Masuda, S., (2012). Light detection and signal transduction in the bluf photoreceptors. *Plant Cell Physiol.* **54**, 171–179.
[22]. Anderson, S. et al, (2005). Structure of a novel photoreceptor, the BLUF domain of AppA from Rhodobacter sphaeroides. *Biochemistry* **44**, 7998–8005.
[23]. Jung, A., Reinstein, J., Domratcheva, T., Shoeman, R.L., Schlichting, I., (2006). Crystal structures of the AppA BLUF domain photoreceptor provide insights into blue light-mediated signal transduction. *J. Mol. Biol.* **362**, 717–732.
[24]. Yuan, H. et al, (2006). Crystal structures of the synechocystis photoreceptor slr1694 reveal distinct structural states related to signaling. *Biochemistry* **45**, 12687–12694.
[25]. Domratcheva, T., Grigorenko, B., Schlichting, I., Nemukhin, A., (2008). Molecular models predict light-induced glutamine tautomerization in bluf photoreceptors. *Biophys. J.* **94**, 3872–3879.
[26]. Winkler, A. et al, (2013). A ternary AppA–PpsR–DNA complex mediates light regulation of photosynthesis-related gene expression. *Nat. Struct. Mol. Biol.* **20**, 859–867.
[27]. Rockwell, N.C., Su, Y.-S., Lagarias, J.C., (2006). Phytochrome structure and signaling mechanisms. *Annu. Rev. Plant Biol.* **57**, 837–858.
[28]. López, M.F. et al, (2022). Photoinduced reaction mechanisms in prototypical and bathy phytochromes. *Phys. Chem. Chem. Phys.* **24**, 11967–11978.
[29]. Escobar, F.V. et al, (2015). A protonation-coupled feedback mechanism controls the signalling process in bathy phytochromes. *Nat. Chem.* **7**, 423–430.
[30]. Burgie, E.S. et al, (2014). Crystallographic and electron microscopic analyses of a bacterial phytochrome reveal local and global rearrangements during photoconversion. *J. Biol. Chem.* **289**, 24573–24587.
[31]. Takala, H. et al, (2014). Signal amplification and transduction in phytochrome photosensors. *Nature* **509**, 245–248.
[32]. Björling, A. et al, (2016). Structural photoactivation of a full-length bacterial phytochrome. *Sci. Adv.* **2**, e1600920.
[33]. Wagner, J.R. et al, (2008). Mutational analysis of deinococcus radiodurans bacteriophytochrome reveals key amino acids necessary for the photochromicity and proton exchange cycle of phytochromes. *J. Biol. Chem.* **283**, 12212–12226.

[34]. Macaluso, V., Cupellini, L., Salvadori, G., Lipparini, F., Mennucci, B., (2020). Elucidating the role of structural fluctuations, and intermolecular and vibronic interactions in the spectroscopic response of a bacteriophytochrome. *Phys. Chem. Chem. Phys.* **22**, 8585–8594.
[35]. Muzzopappa, F., Kirilovsky, D., (2020). Changing color for photoprotection: the orange carotenoid protein. *Trends Plant Sci.* **25**, 92–104.
[36]. Kerfeld, C.A. et al, (2003). The crystal structure of a cyanobacterial water-soluble carotenoid binding protein. *Structure* **11**, 55–65.
[37]. Leverenz, R.L. et al, (2015). A 12 å carotenoid translocation in a photoswitch associated with cyanobacterial photoprotection. *Science* **348**, 1463–1466.
[38]. Domínguez-Martín, M.A. et al, (2022). Structures of a phycobilisome in light-harvesting and photoprotected states. *Nature* **609**, 835–845.
[39]. Konold, P.E. et al, (2018). Photoactivation mechanism, timing of protein secondary structure dynamics and carotenoid translocation in the orange carotenoid protein. *J. Am. Chem. Soc.* **141**, 520–530.
[40]. Terada, T., Kidera, A., (2012). Comparative molecular dynamics simulation study of crystal environment effect on protein structure. *J. Phys. Chem. B* **116**, 6810–6818.
[41]. Takala, H. et al, (2016). Light-induced structural changes in a monomeric bacteriophytochrome. *Struct. Dyn.* **3**, 054701.
[42]. Fujisawa, T., Masuda, S., (2018). Light-induced chromophore and protein responses and mechanical signal transduction of BLUF proteins. *Biophys. Rev.* **10**, 327–337.
[43]. Grinstead, J.S. et al, (2006). The solution structure of the AppA BLUF domain: Insight into the mechanism of light-induced signaling. *Chembiochem* **7**, 187–193.
[44]. Wilson, A. et al, (2010). Structural determinants underlying photoprotection in the photoactive orange carotenoid protein of cyanobacteria. *J. Biol. Chem.* **285**, 18364–18375.
[45]. Hashem, S. et al, (2021). From crystallographic data to the solution structure of photoreceptors: the case of the AppA BLUF domain. *Chem. Sci.* **12**, 13331–13342.
[46]. Götze, J.P., Greco, C., Mitrić, R., Bonačić-Koutecký, V., Saalfrank, P., (2012). BLUF hydrogen network dynamics and UV/vis spectra: A combined molecular dynamics and quantum chemical study. *J. Comput. Chem.* **33**, 2233–2242.
[47]. Obanayama, K., Kobayashi, H., Fukushima, K., Sakurai, M., (2008). Structures of the chromophore binding sites in bluf domains as studied by molecular dynamics and quantum chemical calculations. *Photochem. Photobiol.* **84**, 1003–1010.
[48]. Meier, K., Thiel, W., van Gunsteren, W.F., (2012). On the effect of a variation of the force field, spatial boundary condition and size of the qm region in qm/mm md simulations. *J. Comput. Chem.* **33**, 363–378.
[49]. Hsiao, Y.-W., Götze, J.P., Thiel, W., (2012). The central role of gln63 for the hydrogen bonding network and UV–visible spectrum of the AppA BLUF domain. *J. Phys. Chem. B* **116**, 8064–8073.
[50]. Collette, F., Renger, T., Schmidt am Busch, M., (2014). Revealing the functional states in the active site of BLUF photoreceptors from electrochromic shift calculations. *J. Phys. Chem. B* **118**, 11109–11119.
[51]. Macaluso, V., Salvadori, G., Cupellini, L., Mennucci, B., (2021). The structural changes in the signaling mechanism of bacteriophytochromes in solution revealed by a multiscale computational investigation. *Chem. Sci.* **12**, 5555–5565.
[52]. Bondanza, M., Cupellini, L., Lipparini, F., Mennucci, B., (2020). The multiple roles of the protein in the photoactivation of orange carotenoid protein. *Chem* **6**, 187–203.
[53]. Lorenz-Fonfria, V.A., (2020). Infrared difference spectroscopy of proteins: from bands to bonds. *Chem. Rev.* **120**, 3466–3576.
[54]. Khrenova, M.G., Nemukhin, A.V., Grigorenko, B.L., Krylov, A.I., Domratcheva, T.M., (2010). Quantum chemistry calculations provide support to the mechanism of the light-induced structural changes in the flavin-binding photoreceptor proteins. *J. Chem. Theory Comput.* **6**, 2293–2302.
[55]. Ihalainen, J.A. et al, (2018). Chromophore–protein interplay during the phytochrome photocycle revealed by step-scan FTIR spectroscopy. *J. Am. Chem. Soc.* **140**, 12396–12404.
[56]. Macaluso, V. et al, (2021). Ultrafast transient infrared spectroscopy of photoreceptors with polarizable QM/MM dynamics. *J. Phys. Chem. B* **125**, 10282–10292.
[57]. Brust, R. et al, (2013). Proteins in action: femtosecond to millisecond structural dynamics of a photoactive flavoprotein. *J. Am. Chem. Soc.* **135**, 16168–16174.
[58]. Senn, H.M., Thiel, W., (2009). QM/MM methods for biomolecular systems. *Angew. Chem. Int. Ed.* **48**, 1198–1229.
[59]. Lin, H., Truhlar, D.G., (2006). Qm/mm: what have we learned, where are we, and where do we go from here? *Theor. Chem. Acc.* **117**, 185.
[60]. Nochebuena, J., Naseem-Khan, S., Cisneros, G.A., (2021). Development and application of quantum mechanics/molecular mechanics methods with advanced polarizable potentials. *Wiley Interdiscip. Rev. Comput. Mol. Sci.* **11**
[61]. Nottoli, M. et al, (2023). QM/AMOEBA description of properties and dynamics of embedded molecules. *Wiley Interdiscip. Rev. Comput. Mol. Sci.*
[62]. Rappe, A., Goddard, W., (1991). Charge equilibration for molecular-dynamics simulations. *J. Phys. Chem.* **95**, 3358–3363.
[63]. Rick, S.W., Stuart, S.J., Berne, B.J., (1994). Dynamical fluctuating charge force fields: application to liquid water. *J. Chem. Phys.* **101**, 6141–6156.
[64]. Lipparini, F., Barone, V., (2011). Polarizable force fields and polarizable continuum model: a fluctuating charges/PCM approach. 1. Theory and implementation. *J. Chem. Theory Comput.* **7**, 3711–3724.
[65]. Poier, P.P., Jensen, F., (2019). Describing molecular polarizability by a bond capacity model. *J. Chem. Theory Comput.* **15**, 3093–3107.
[66]. Cappelli, C., (2016). Integrated QM/polarizable MM/continuum approaches to model chiroptical properties of strongly interacting solute–solvent systems. *Int. J. Quantum Chem.* **116**, 1532–1542.
[67]. Boulanger, E., Thiel, W., (2012). Solvent boundary potentials for hybrid QM/MM computations using classical drude oscillators: a fully polarizable model. *J. Chem. Theory Comput.* **8**, 4527–4538.

[68]. Riahi, S., Rowley, C.N., (2014). The CHARMM-TURBOMOLE interface for efficient and accurate QM/MM molecular dynamics, free energies, and excited state properties. *J. Comput. Chem.* **35**, 2076–2086.
[69]. Warshel, A., Levitt, M., (1976). Theoretical studies of enzymic reactions: dielectric, electrostatic and steric stabilization of the carbonium ion in the reaction of lysozyme. *J. Mol. Biol.* **103**, 227–249.
[70]. Applequist, J., Carl, J.R., Fung, K.-K., (1972). Atom dipole interaction model for molecular polarizability. Application to polyatomic molecules and determination of atom polarizabilities. *J. Am. Chem. Soc.* **94**, 2952–2960.
[71]. Thole, B.T., (1981). Molecular polarizabilities calculated with a modified dipole interaction. *Chem. Phys.* **59**, 341.
[72]. Thompson, M.A., Schenter, G.K., (1995). Excited states of the bacteriochlorophyll b dimer of Rhodopseudomonas viridis: a QM/MM study of the photosynthetic reaction center that includes MM polarization. *J. Phys. Chem.* **99**, 6374–6386.
[73]. Gao, J., (1997). Energy components of aqueous solution: insight from hybrid QM/MM simulations using a polarizable solvent model. *J. Comput. Chem.* **18**, 1061–1071.
[74]. Curutchet, C. et al, (2009). Electronic energy transfer in condensed phase studied by a polarizable QM/MM model. *J. Chem. Theory Comput.* **5**, 1838–1848.
[75]. Olsen, J.M.H. & Kongsted, J. Chapter 3 - molecular properties through polarizable embedding. vol. 61 of Adv. Quantum Chem., 107–143 (Academic Press, 2011).
[76]. Dziedzic, J. et al, (2016). Tinktep: a fully self-consistent, mutually polarizable QM/MM approach based on the AMOEBA force field. *J. Chem. Phys.* **145**, 124106.
[77]. Wu, X. et al, (2017). Simulating electron dynamics in polarizable environments. *J. Chem. Theory Comput.* **13**, 3985–4002.
[78]. Loco, D. et al, (2019). Towards large scale hybrid QM/MM dynamics of complex systems with advanced point dipole polarizable embeddings. *Chem. Sci.* **10**, 7200–7211.
[79]. Dreuw, A., Head-Gordon, M., (2005). Single-reference ab initio methods for the calculation of excited states of large molecules. *Chem. Rev.* **105**, 4009–4037.
[80]. Izsák, R., (2019). Single-reference coupled cluster methods for computing excitation energies in large molecules: the efficiency and accuracy of approximations. *WIREs Comput. Mol. Sci.* **10**
[81]. Thiel, W., (2013). Semiempirical quantum-chemical methods. *WIREs Comput. Mol. Sci.* **4**, 145–157.
[82]. Persico, M., Granucci, G., (2014). An overview of nonadiabatic dynamics simulations methods, with focus on the direct approach versus the fitting of potential energy surfaces. *Theor. Chem. Acc.* **133**, 1526–1528.
[83]. Dral, P.O. et al, (2016). Semiempirical quantum-chemical orthogonalization-corrected methods: theory, implementation, and parameters. *J. Chem. Theory Comput.* **12**, 1082–1096.
[84]. Seifert, G., Joswig, J.-O., (2012). Density-functional tight binding – an approximate density-functional theory method. *WIREs Comput. Mol. Sci.* **2**, 456–465.
[85]. Gilbert, A.T.B., Besley, N.A., Gill, P.M.W., (2008). Self-consistent field calculations of excited states using the maximum overlap method (MOM). *J. Phys. Chem. A* **112**, 13164–13171.
[86]. Barca, G.M.J., Gilbert, A.T.B., Gill, P.M.W., (2018). Simple models for difficult electronic excitations. *J. Chem. Theory Comput.* **14**, 1501–1509.
[87]. Carter-Fenk, K., Herbert, J.M., (2020). State-targeted energy projection: a simple and robust approach to orbital relaxation of non-aufbau self-consistent field solutions. *J. Chem. Theory Comput.* **16**, 5067–5082.
[88]. Hait, D., Head-Gordon, M., (2021). Orbital Optimized Density Functional Theory for Electronic Excited States. *J. Phys. Chem. Lett.* **12**, 4517–4529.
[89]. Lischka, H. et al, (2018). Multireference approaches for excited states of molecules. *Chem. Rev.* **118**, 7293–7361.
[90]. Strambi, A., Durbeej, B., Ferré, N., Olivucci, M., (2010). Anabaena sensory rhodopsin is a light-driven unidirectional rotor. *Proc. Natl. Acad. Sci. USA* **107**, 21322–21326.
[91]. Altoè, P., Cembran, A., Olivucci, M., Garavelli, M., (2010). Aborted double bicycle-pedal isomerization with hydrogen bond breaking is the primary event of bacteriorhodopsin proton pumping. *Proc. Natl. Acad. Sci. USA* **107**, 20172–20177.
[92]. Schapiro, I. et al, (2011). The ultrafast photoisomerizations of rhodopsin and bathorhodopsin are modulated by bond length alternation and hoop driven electronic effects. *J. Am. Chem. Soc.* **133**, 3354–3364.
[93]. Rinaldi, S., Melaccio, F., Gozem, S., Fanelli, F., Olivucci, M., (2014). Comparison of the isomerization mechanisms of human melanopsin and invertebrate and vertebrate rhodopsins. *Proc. Natl. Acad. Sci. USA* **111**, 1714–1719.
[94]. Luk, H.L., Melaccio, F., Rinaldi, S., Gozem, S., Olivucci, M., (2015). Molecular bases for the selection of the chromophore of animal rhodopsins. *Proc. Natl. Acad. Sci. USA* **112**, 15297–15302.
[95]. Dokukina, I., Weingart, O., (2015). Spectral properties and isomerisation path of retinal in c1c2 channelrhodopsin. *Phys. Chem. Chem. Phys.* **17**, 25142–25150.
[96]. Hontani, Y. et al, (2017). Reaction dynamics of the chimeric channelrhodopsin C1C2. *Sci. Rep.* **7**, 7217.
[97]. Chang, X.-P., Gao, Y.-J., Fang, W.-H., Cui, G., Thiel, W., (2017). Quantum mechanics/molecular mechanics study on the photoreactions of dark- and light-adapted states of a blue-light ytva lov photoreceptor. *Angew. Chem. Int. Ed.* **56**, 9341–9345.
[98]. Liu, X.-Y. et al, (2021). Hydrogen-bond network determines the early photoisomerization processes of Cph1 and AnPixJ phytochromes. *Angew. Chem. Int. Ed.* **60**, 18688–18693.
[99]. Wei, L., Wang, H., Chen, X., Fang, W., Wang, H., (2014). A comprehensive study of isomerization and protonation reactions in the photocycle of the photoactive yellow protein. *Phys. Chem. Chem. Phys.* **16**, 25263–25272.
[100]. Zhang, T.-S., Fang, Y.-G., Song, X.-F., Fang, W.-H., Cui, G., (2020). Hydrogen-bonding interaction regulates photoisomerization of a single-bond-rotation locked photoactive yellow protein chromophore in protein. *J. Phys. Chem. Lett.* **11**, 2470–2476.

[101]. Durbeej, B., (2009). On the primary event of phytochrome: quantum chemical comparison of photoreactions at C4, C10 and C15. *Phys. Chem. Chem. Phys.* **11**, 1354–1361.
[102]. Strambi, A., Durbeej, B., (2011). Initial excited-state relaxation of the bilin chromophores of phytochromes: a computational study. *Photochem. Photobiol. Sci.* **10**, 569–579.
[103]. Falklöf, O., Durbeej, B., (2016). Steric effects govern the photoactivation of phytochromes. *ChemPhysChem* **17**, 954–957.
[104]. Gromov, E.V., Burghardt, I., Köppel, H., Cederbaum, L. S., (2011). Photoinduced isomerization of the photoactive yellow protein (PYP) chromophore: Interplay of two torsions, a HOOP mode and hydrogen bonding. *J. Phys. Chem. A* **115**, 9237–9248.
[105]. Gromov, E.V., (2014). Unveiling the mechanism of photoinduced isomerization of the photoactive yellow protein (PYP) chromophore. *J. Chem. Phys.* **141**
[106]. Bondanza, M., Jacquemin, D., Mennucci, B., (2021). Excited states of xanthophylls revisited: toward the simulation of biologically relevant systems. *J. Phys. Chem. Lett.* **12**, 6604–6612.
[107]. Altoè, P. et al, (2009). Deciphering intrinsic deactivation/isomerization routes in a phytochrome chromophore model. *J. Phys. Chem. B* **113**, 15067–15073.
[108]. Rao, A.G., Schapiro, I., (2022). Photoisomerization of phytochrome chromophore models: an xms-caspt2 study. *Phys. Chem. Chem. Phys.* **24**, 29393–29405.
[109]. Nottoli, M., Mennucci, B., Lipparini, F., (2020). Excited state born–oppenheimer molecular dynamics through coupling between time dependent DFT and AMOEBA. *Phys. Chem. Chem. Phys.* **22**, 19532–19541.
[110]. Loco, D. et al, (2016). A QM/MM approach using the AMOEBA polarizable embedding: from ground state energies to electronic excitations. *J. Chem. Theory Comput.* **12**, 3654–3661.
[111]. Goings, J.J., Hammes-Schiffer, S., (2019). Early photocycle of slr1694 blue-light using flavin photoreceptor unraveled through adiabatic excited-state quantum mechanical/molecular mechanical dynamics. *J. Am. Chem. Soc.* **141**, 20470–20479.
[112]. Goings, J.J., Li, P., Zhu, Q., Hammes-Schiffer, S., (2020). Formation of an unusual glutamine tautomer in a blue light using flavin photocycle characterizes the light-adapted state. *Proc. Natl. Acad. Sci.* **117**, 26626–26632.
[113]. Mazzeo, P., Hashem, S., Lipparini, F., Cupellini, L., Mennucci, B., (2023). Fast method for excited-state dynamics in complex systems and its application to the photoactivation of a blue light using flavin photoreceptor. *J. Phys. Chem. Lett.* **14**, 1222–1229.
[114]. Toh, K. et al, (2008). On the signaling mechanism and the absence of photoreversibility in the AppA BLUF domain. *Biophys. J.* **95**, 312–321.
[115]. Salvadori, G. et al, (2022). Protein control of photochemistry and transient intermediates in phytochromes. *Nat. Commun.* **13**, 6838.
[116]. Tully, J.C., (2012). Perspective: nonadiabatic dynamics theory. *J. Chem. Phys.* **137**, 22A301–22A307.
[117]. Curchod, B.F.E., Martínez, T.J., (2018). Ab initio nonadiabatic quantum molecular dynamics. *Chem. Rev.* **118**, 3305–3336.
[118]. Crespo-Otero, R., Barbatti, M., (2018). Recent advances and perspectives on nonadiabatic mixed quantum-classical dynamics. *Chem. Rev.* **118**, 7026–7068.
[119]. Tully, J.C., (1990). Molecular dynamics with electronic transitions. *J. Chem. Phys.* **93**, 1061–1071.
[120]. Granucci, G., Persico, M., Zoccante, A., (2010). Including quantum decoherence in surface hopping. *J. Chem. Phys.* **133**, 134111/1–134111/9.
[121]. Persico, M., Granucci, G., Accomasso, D., (2022). The quantum decoherence problem in nonadiabatic trajectory methods. *Reference Module in Chemistry, Molecular Sciences and Chemical Engineering*. Elsevier.
[122]. Groenhof, G. et al, (2004). Photoactivation of the photoactive yellow protein: why photon absorption triggers a trans-to-cis isomerization of the chromophore in the protein. *J. Am. Chem. Soc.* **126**, 4228–4233.
[123]. Frutos, L.M., Andruniów, T., Santoro, F., Ferré, N., Olivucci, M., (2007). Tracking the excited-state time evolution of the visual pigment with multiconfigurational quantum chemistry. *Proc. Natl. Acad. Sci. USA* **104**, 7764–7769.
[124]. Polli, D. et al, (2010). Conical intersection dynamics of the primary photoisomerization event in vision. *Nature* **467**, 440–443.
[125]. Polli, D. et al, (2014). Wavepacket splitting and two-pathway deactivation in the photoexcited visual pigment isorhodopsin. *Angew. Chem. Int. Ed.* **53**, 2504–2507.
[126]. Yang, X. et al, (2022). Quantum–classical simulations of rhodopsin reveal excited-state population splitting and its effects on quantum efficiency. *Nat. Chem.* **14**, 441–449.
[127]. Dokukina, I., Nenov, A., Garavelli, M., Marian, C.M., Weingart, O., (2019). QM/MM photodynamics of retinal in the channelrhodopsin chimera c1c2 with OM3/MRCI. *ChemPhotoChem* **3**, 107–116.
[128]. Arcidiacono, A., Accomasso, D., Cupellini, L., Mennucci, B., (2023). How orange carotenoid protein controls the excited state dynamics of canthaxanthin. *Chem. Sci.* **14**, 11158–11169. https://doi.org/10.1039/D3SC02662K.
[129]. Groenhof, G., Schäfer, L.V., Boggio-Pasqua, M., Grubmüller, H., Robb, M.A., (2008). Arginine52 controls the photoisomerization process in photoactive yellow protein. *J. Am. Chem. Soc.* **130**, 3250–3251.
[130]. Morozov, D., Modi, V., Mironov, V., Groenhof, G., (2022). The photocycle of bacteriophytochrome is initiated by counterclockwise chromophore isomerization. *J. Phys. Chem. Lett.* **13**, 4538–4542.
[131]. Ben-Nun, M., Quenneville, J., Martínez, T.J., (2000). Ab initio multiple spawning: photochemistry from first principles quantum molecular dynamics. *J. Phys. Chem. A* **104**, 5161–5175.
[132]. Liang, R., Liu, F., Martínez, T.J., (2019). Nonadiabatic photodynamics of retinal protonated Schiff base in Channelrhodopsin 2. *J. Phys. Chem. Lett.* **10**, 2862–2868.
[133]. Punwong, C., Hannongbua, S., Martínez, T.J., (2019). Electrostatic influence on photoisomerization in bacteriorhodopsin and halorhodopsin. *J. Phys. Chem. B* **123**, 4850–4857.
[134]. Yu, J.K., Liang, R., Liu, F., Martínez, T.J., (2019). First-principles characterization of the elusive I fluorescent state and the structural evolution of retinal protonated Schiff base in Bacteriorhodopsin. *J. Am. Chem. Soc.* **141**, 18193–18203.

[135]. Liang, R., Yu, J.K., Meisner, J., Liu, F., Martinez, T.J., (2021). Electrostatic control of photoisomerization in Channelrhodopsin 2. *J. Am. Chem. Soc.* **143**, 5425–5437.
[136]. Ko, C., Virshup, A.M., Martínez, T.J., (2008). Electrostatic control of photoisomerization in the photoactive yellow protein chromophore: ab initio multiple spawning dynamics. *Chem. Phys. Lett.* **460**, 272–277.
[137]. Virshup, A.M. et al, (2009). Photodynamics in complex environments: ab initio multiple spawning quantum mechanical/molecular mechanical dynamics. *J. Phys. Chem. B* **113**, 3280–3291.
[138]. Jones, C.M., List, N.H., Martínez, T.J., (2021). Resolving the ultrafast dynamics of the anionic green fluorescent protein chromophore in water. *Chem. Sci.* **12**, 11347–11363.
[139]. List, N.H., Jones, C.M., Martínez, T.J., (2022). Internal conversion of the anionic GFP chromophore: in and out of the I-twisted S1/S0 conical intersection seam. *Chem. Sci.* **13**, 373–385.
[140]. Liu, R.S.H., (2001). Photoisomerization by hula-twist: a fundamental supramolecular photochemical reaction. *Acc. Chem. Res.* **34**, 555–562.
[141]. Liu, R.S.H., Hammond, G.S., (2000). The case of medium-dependent dual mechanisms for photoisomerization: one-bond-flip and hula-twist. *Proc. Natl. Acad. Sci. USA* **97**, 11153–11158.
[142]. Fadini, A. et al, (2023). Serial femtosecond crystallography reveals that photoactivation in a fluorescent protein proceeds via the hula twist mechanism. *J. Am. Chem. Soc.* **145**, 15796–15808.
[143]. Zhang, Q., Chen, X., Cui, G., Fang, W.-H., Thiel, W., (2014). Concerted asynchronous hula-twist photoisomerization in the s65t/h148d mutant of green fluorescent protein. *Angew. Chem.* **126**, 8793–8797.
[144]. Chenchiliyan, M. et al, (2023). Ground-state heterogeneity and vibrational energy redistribution in bacterial phytochrome observed with femtosecond 2d IR spectroscopy. *J. Chem. Phys.* **158**
[145]. Hashem, S., Alteri, G.B., Cupellini, L., Mennucci, B., (2023). Integrated computational study of the light-activated structure of the AppA BLUF domain and its spectral signatures. *J. Phys. Chem. A* **127**, 5065–5074.
[146]. Bussi, G., Laio, A., (2020). Using metadynamics to explore complex free-energy landscapes. *Nat. Rev. Phys.* **2**, 200–212.
[147]. Barducci, A., Bonomi, M., Parrinello, M., (2011). Metadynamics. *Wiley Interdiscip. Rev. Comput. Mol. Sci.* **1**, 826–843.
[148]. Pfaendtner, J., (2019). Metadynamics to enhance sampling in biomolecular simulations. *In: Methods in Molecular Biology*. Springer, New York, pp. 179–200.
[149]. Valsson, O., Tiwary, P., Parrinello, M., (2016). Enhancing important fluctuations: Rare events and metadynamics from a conceptual viewpoint. *Annu. Rev. Phys. Chem.* **67**, 159–184.
[150]. Bernardi, R.C., Melo, M.C., Schulten, K., (2015). Enhanced sampling techniques in molecular dynamics simulations of biological systems. *Biochim. Biophys. Acta (bba) - Gen. Subj.* **1850**, 872–877.
[151]. Miao, Y., McCammon, J.A., (2016). Unconstrained enhanced sampling for free energy calculations of biomolecules: a review. *Mol. Simul.* **42**, 1046–1055.
[152]. Torrie, G., Valleau, J., (1977). Nonphysical sampling distributions in monte carlo free-energy estimation: Umbrella sampling. *J. Comput. Phys.* **23**, 187–199.
[153]. Laio, A., Parrinello, M., (2002). Escaping free-energy minima. *Proc. Natl. Acad. Sci. USA* **99**, 12562–12566.
[154]. Barducci, A., Bussi, G., Parrinello, M., (2008). Well-tempered metadynamics: a smoothly converging and tunable free-energy method. *Phys. Rev. Lett.* **100**, 020603.
[155]. Valsson, O., Parrinello, M., (2014). Variational approach to enhanced sampling and free energy calculations. *Phys. Rev. Lett.* **113**
[156]. Rydzewski, J., Walczewska-Szewc, K., Czach, S., Nowak, W., Kuczera, K., (2022). Enhancing the inhomogeneous photodynamics of canonical bacteriophytochrome. *J. Phys. Chem. B* **126**, 2647–2657.
[157]. Mills, G., Jónsson, H., Schenter, G.K., (1995). Reversible work transition state theory: application to dissociative adsorption of hydrogen. *Surf. Sci.* **324**, 305–337.
[158]. Dickson, B.M., Huang, H., Post, C.B., (2012). Unrestrained computation of free energy along a path. *J. Phys. Chem. B* **116**, 11046–11055.
[159]. Goings, J.J., Reinhardt, C.R., Hammes-Schiffer, S., (2018). Propensity for proton relay and electrostatic impact of protein reorganization in Slr1694 BLUF Photoreceptor. *J. Am. Chem. Soc.* **140**, 15241–15251.
[160]. Goyal, P., Hammes-Schiffer, S., (2017). Role of active site conformational changes in photocycle activation of the AppA BLUF photoreceptor. *Proc. Natl. Acad. Sci. USA* **114**, 1480–1485.
[161]. Branduardi, D., Gervasio, F.L., Parrinello, M., (2007). From a to b in free energy space. *J. Chem. Phys.* **126**
[162]. Leines, G.D., Ensing, B., (2012). Path finding on high-dimensional free energy landscapes. *Phys. Rev. Lett.* **109**
[163]. de Alba Ortíz, A.P., Rovira, C., Ensing, B., (2023). Free energies of the gln tautomerization and rotation mechanism of dark-state recovery in blue light-using flavin proteins. *bioRxiv*.
[164]. Abrams, C., Bussi, G., (2013). Enhanced sampling in molecular dynamics using metadynamics, replica-exchange, and temperature-acceleration. *Entropy* **16**, 163–199.
[165]. Earl, D.J., Deem, M.W., (2005). Parallel tempering: theory, applications, and new perspectives. *Phys. Chem. Chem. Phys.* **7**, 3910–3916.
[166]. Hansmann, U.H., (1997). Parallel tempering algorithm for conformational studies of biological molecules. *Chem. Phys. Lett.* **281**, 140–150.
[167]. Ganguly, A., Thiel, W., Crane, B.R., (2017). Glutamine amide flip elicits long distance allosteric responses in the LOV protein vivid. *J. Am. Chem. Soc.* **139**, 2972–2980.
[168]. Bondanza, M., Cupellini, L., Faccioli, P., Mennucci, B., (2020). Molecular mechanisms of activation in the orange carotenoid protein revealed by molecular dynamics. *J. Am. Chem. Soc.* **142**, 21829–21841.
[169]. Jumper, J. et al, (2021). Highly accurate protein structure prediction with AlphaFold. *Nature* **596**, 583–589.
[170]. Akdel, M. et al, (2022). A structural biology community assessment of AlphaFold2 applications. *Nat. Struct. Mol. Biol.* **29**, 1056–1067.

[171]. Kulichenko, M. et al, (2021). The rise of neural networks for materials and chemical dynamics. *J. Phys. Chem. Lett.* **12**, 6227–6243.
[172]. Unke, O.T. et al, (2021). Machine learning force fields. *Chem. Rev.* **121**, 10142–10186.
[173]. Keith, J.A. et al, (2021). Combining machine learning and computational chemistry for predictive insights into chemical systems. *Chem. Rev.* **121**, 9816–9872.
[174]. Westermayr, J., Marquetand, P., (2021). Machine learning for electronically excited states of molecules. *Chem. Rev.* **121**, 9873–9926.
[175]. Richings, G.W., Habershon, S., (2022). Predicting molecular photochemistry using machine-learning-enhanced quantum dynamics simulations. *Acc. Chem. Res.* **55**, 209–220.
[176]. Raghavan, B. et al, (2023). Drug design in the exascale era: A perspective from massively parallel QM/MM simulations. *J. Chem. Inf. Model* **63**, 3647–3658.
[177]. Wieczór, M. et al, (2023). Pre-exascale hpc approaches for molecular dynamics simulations.covid-19 research: A use case. *WIREs Comput. Mol. Sci.* **13**, e1622.